

Evangelos Karagiannis

Numerical Simulation of Submarine Slides in Bjørnafjorden Using Rheological Models

June 2019



Norwegian University of
Science and Technology

Numerical Simulation of Submarine Slides in Bjørnafjorden Using Rheological Models

Evangelos Karagiannis

Geotechnics and Geohazards

Submission date: June 2019

Supervisor: Professor Vikas Thakur

Co-supervisor: Dr. Samson A. Degago, SV

Norwegian University of Science and Technology
Department of Civil and Environmental Engineering

Thesis Title: <i>Numerical Simulation of Submarine Slides in Bjørnafjorden Using Rheological Models</i>	Date: <i>June 9th, 2019</i> Number of pages (with appendix): 86				
	<table border="1" style="margin: auto; border-collapse: collapse;"> <tr> <td style="padding: 5px;">Master Thesis</td> <td style="padding: 5px; text-align: center;">X</td> <td style="padding: 5px;">Project work</td> <td style="width: 20px;"></td> </tr> </table>	Master Thesis	X	Project work	
Master Thesis	X	Project work			
Name: <i>EVANGELOS KARAGIANNIS</i>					
Professor in charge/Supervisor: <i>PROFESSOR VIKAS THAKUR</i>					
Other external professional contacts/Supervisors: <i>Dr. SANSON A. DEGAGO, SVV</i>					
Abstract <p>The continuous development of the world creates the need for submarine transport and communication. Consequently, seafloor instabilities may create complications in the everyday life of humans. A sustainable design for the lifespan of urban infrastructure is vital for the maintenance of their operation. Statens Vegvesen aims at the completion of the E39 project without having any ferry connections. In the context of E39, a side-anchored floating bridge will be constructed in Bjørnafjorden, and the mooring system will be anchored on the seabed.</p> <p>In the first part, the definition of the problem is given together with the description of the geological situation of Bjørnafjorden's seafloor. Subsequently, a literature review is provided on landslides. Additionally, a brief description of the mathematical background of DAN3D is included.</p> <p>The stability of the seafloor is a crucial element of the study, and an extensive back-calculation for the determination of the governing geotechnical and rheological parameters is detailed. All the analyses were conducted with the software DAN3D. This study approaches the topic from different aspects. Several empirical approaches are adopted in order to estimate the run-out distance of a given landslide. In the numerical analysis, two rheological models are chosen for the back-calculation of the landslide. Both plastic and frictional rheologies simulate the landslide in a realistic way.</p> <p>Finally, a comparison with NGI's conclusions is conducted to confirm the correctness of the present study and give a clear overview of the geotechnical conditions in Bjørnafjorden's seabed. The study concludes with recommendations and suggestions on future work based on the simulation results.</p>					

Keywords

1. Run-Out Distance
2. Plastic Rheological Model
3. Frictional Rheological Model
4. Submarine Landslides
5. DAN3D

Preface

The present Master Thesis is submitted as the final requirement for the completion of the Master's Degree (MSc) in "Geotechnics and Geohazards" at the Geotechnical Division of the Civil and Environmental Engineering Department of the Norwegian University of Science and Technology (NTNU). The study was carried out during the spring semester of 2019.

A literature review concerning landslides, empirical approaches concerning the calculation of the run-out distance and numerical simulations for the back-calculation of a landslide are included in the present Master Thesis.

Acknowledgments

First of all, I would like to thank my supervisor, Professor Vikas Thakur, for his guidance both throughout the Master's Degree and during our cooperation at the present master thesis. The understanding that he showed and the multifaceted assistance, when I needed, was significant. I would like also to thank Kenneth Sundli for installing DAN3D software and making it available anytime that I needed it.

In the sequel, I would like to express my deepest gratitude to Dr. Samson A. Degago for his guidance and his feedback during my thesis. Without his help, the completion of the present master thesis would be impossible. The suggestions that he provide me played a fundamental role. I would like also to thank Heidi Kjennbakken for providing me with all the necessary data for the study of the stability of Bjørnafjorden seafloor.

Of course, it would be an omission not to thank Mr. Ashenafi L. Yifru, Ph.D. candidate at the Geotechnical Division of the Civil and Environmental Engineering Department, for the time that he dedicated for explaining me how does DAN3D work. Additionally, my special thanks go to all of my friends who helped me proofread my thesis. Their feedback was useful and constructive.

Last but not least, the biggest thank you should go to my parents and siblings for their mental and phycological support. They were always taking care of me and I would not be able to achieve anything without them.

Evangelos Karagiannis

Table of Contents

Abstract.....	Σφάλμα! Δεν έχει οριστεί σελιδοδείκτης.
Preface	iii
Acknowledgments.....	v
Table of Contents.....	vii
List of Figures.....	ix
List of Tables	xi
List of Symbols.....	xiii
1. Introduction.....	1
2. Description.....	3
2.1. General Background	3
2.2. The Main Objective of the Study.....	5
2.3. Outline of the thesis	6
3. Literature Report.....	7
3.1. Introduction.....	7
3.2. Definition	7
3.3. Characteristics of Landslides	8
3.4. Classification of landslides	10
3.3.1. Falls.....	13
3.3.2. Topples.....	13
3.3.3. Slides.....	13
3.3.4. Spreads.....	14
3.3.5. Flows.....	14
3.3.6. Complex.....	15
3.5. Submarine Landslides.....	15
4. Mathematical Background and Equations behind Rheological Models.....	17
4.1. DAN3D Model.....	17
4.2. Concept of “ <i>Equivalent Fluid</i> ”	18
4.3. Governing Equations	19
4.4. Basal Rheological Models	24
5. Simulation Results of the Models	27
5.1. Introduction.....	27
5.2. Empirical Approach	28
5.3. Procedure for Simulations using DAN3D Models.....	34
5.4. Methodology of Analysis.....	37
5.5. Results.....	44

5.5.1.	Plastic Rheological Model	45
5.5.2.	Frictional Rheological Model	51
5.6.	Comparison with NGI's Results	54
5.6.1.	Description of BING's Model.....	54
5.6.2.	Parameters of BING's Model	55
5.6.3.	Comparison of Models.....	56
6.	Discussion of Results.....	59
6.1.	Introduction.....	59
6.2.	Empirical Approach	59
6.3.	Numerical Calculation of Run-Out Distance	60
6.3.1.	Plastic Rheological Model	60
6.3.2.	Frictional Rheological Model	61
6.4.	Comparison of Models.....	62
7.	Conclusions and Recommendations for Further Work	63
7.1.	Conclusions.....	63
7.2.	Further Work.....	65
7.3.	Recommendations.....	65
	REFERNCES	67
	APPENDIX.....	71

List of Figures

Figure 1: Simplified illustration of the glacial history in Bjørnafjorden, similar to all western Norwegian fjords. The sketch shows the maximum point of the glacier, glacial marine sediments' deposition, the progress of Younger Dryas and the mass deposits at the post-glacial period.....	4
Figure 2: Graphical illustration of the main characteristics of an ideal landslide.....	9
Figure 3: Classification according to Hungr, Leroueil et al. (2014). Landslides are separated based on the movement type and the material which is involved in it.....	12
Figure 4: Graphical illustration of mass movements made of solid and water mixtures at various stages of mixing proposed by Meunier (1993).	16
Figure 5: Illustration of the semi-empirical approach of "Equivalent Fluid".	18
Figure 6: Total Stresses situation on a landslide's material particle. They are also visible in the directions of z- and x-axes.	21
Figure 7: Normalizing coefficients on total stress situation on a landslide's material particle. Stress coefficients are considered positive.	23
Figure 8: Typical Section shows the Height (H) and the Length (L) of a debris flow. Both height and length are measured from the crown until the farthest edge of the landslide's deposit in the vertical and horizontal directions respectively.....	29
Figure 9: Graphical illustration of the approach of the empirical expression which can be used for debris flows, rotational or translational slides and rock falls.....	30
Figure 10: Graphical illustration of the approach of an empirical equation developed for debris flows.	31
Figure 11: Graphical illustration of the approach of an empirical equation developed for landslides caused by earthquakes.....	32
Figure 12: Graphical illustration of the approach of an empirical equation developed for debris flows. The run-out distance is calculated based on the sliding mass' volume.....	33
Figure 13: A typical cross-section of how does the "Source Depth" topography file look like	34
Figure 14: The white lines are the original contours, the green the new contours and the area (marked with yellow lines) multiplied with the contour difference can give a volume approximation.....	35
Figure 15: The white lines are the original contours, the green the new contours and the purple represent the height contours passing where the original and the new contours are intersecting because the height on those points is known.	36
Figure 16: Procedure and Flow Chart for the DAN3D Model Simulations.....	37
Figure 17: Black line shows a typical section of how the topography at the "Path Topography" file should look like and the green and red line represent the sliding mass at the release and final deposition area respectively.....	38
Figure 18: DAN3D Input Parameters using Plastic Rheological Model (left) and Frictional Rheological Model (right).....	39
Figure 19: Every group of lines can be considered as an individual line because no matter what the internal friction angle is, the run-out distance is not affected so much. Parameters like shear strength and unit weight play a more significant role at the determination of the final result.	40
Figure 20: Linear increase of the remoulded shear strength with depth.	41
Figure 21: "Control Parameter" (left) and "Grid File Assignment" (right) dialog boxes.	43
Figure 22: "Data Output Options" dialog box. The "Parameters" tab (left) shows the location of the saved output files and the "Output Files" tab (right) shows the selected output files.	43
Figure 23: "Options" dialog box showing the values which have been used for the simulations.	44
Figure 24: (Left) Geomorphology of submarine landslide (Bjørnafjorden, Norway). The black line separates the release area with the final deposition area. (Right) The original shape of the landslide as it is shown in NGI (2017).....	46

Figure 25: Comparison of the run-out distances of the two alternative topographies. 47

Figure 26: Comparison of the maximum velocity and how it evolves with time in both alternative topographies. 47

Figure 27: Comparison of the average thickness and how it evolves with time in both alternative topographies. 48

Figure 28: Landslide progression on the 1st Topography alternative. Flow thickness contours at 0, 3, 5, 7, 9, 12, 15 and 25 simulation time (seconds) using plastic rheology. Legends show the thickness of the landslide (left) and the elevation (right). The red dashed line shows the limits of the actual deposition of the landslide. 49

Figure 29: Landslide progression on the 2nd Topography alternative. Flow thickness contours at 0, 3, 5, 7, 10, 13, 17 and 25 simulation time (seconds) using plastic rheology. Legends show the thickness of the landslide (left) and the elevation (right). The red dashed line shows the limits of the actual deposition of the landslide. 50

Figure 30: Comparison of the run-out distances with the frictional rheological model. 51

Figure 31: Comparison of the maximum velocity between the plastic and the frictional rheological model. 52

Figure 32: Comparison of the average thickness between the plastic and the frictional rheological model. 52

Figure 33: Landslide progression with the frictional rheological model. Flow thickness contours at 0, 5, 8, 12, 16, 20, 24 and 40 simulation time (seconds) using plastic rheology. Legends show the landslide's thickness (left) and the elevation (right). The red dashed line shows the limits of the actual deposition of the landslide. 53

Figure 34: This drawing shows the components of a debris model. The Shear layer is at the bottom of the flow and the plug layer is above and plowing the slip plane. 55

Figure 35: Landslide progression on the 2nd Topography alternative. Flow thickness contours at 0, 10, 15, 25, 35, 40, 50 and 70 simulation time (seconds) using plastic rheology. Legends show the landslide's thickness (left) and the elevation (right). The red dashed line shows the limits of the actual deposition of the landslide. 57

Figure 36: Comparison of the maximum velocity between the plastic, the frictional rheology, and the BING3 model. 58

Figure 37: Comparison of the average thickness between the plastic, the frictional rheology, and the BING3 model. 58

List of Tables

Table 1: The values of the parameters which have been used for the back-calculation of the landslide. With bold the values which gave the best fit.	45
Table 2: The values of the parameters which have been used for the back-calculation of the landslide. With bold the values which gave the best fit.	51
Table 3: Best-fit parameters for the landslide back-analysis from NGI's back-calculation.	55
Table 4: Table with the proposed values of the parameters which gave the most representative and realistic results in both rheological models.	64

List of Symbols

Roman Letters

c	Cohesion
C	Constant
C_{FR}	Friction Drag Coefficient
C_p	Pressure Drag Coefficient
f	Friction Coefficient
g	Gravitational Acceleration
h	Bed-Normal Flow Thickness
H	Height
k	Pressure Coefficient
L	Run-Out Distance
n	Herschel-Bulkley Exponent
R	Bed-Normal Curvature Radius
R^2	Coefficient of Determination
R_u	Pore-Pressure Coefficient
S_u	Shear Strength
$S_{u_{rem}}$	Remoulded Shear Strength
T	Stress Tensor
u	Pore Pressure
v	Velocity Vector
V	Volume

Greek Letters

α	Inclination of the Bed from Horizontal in Degrees
γ	Unit Weight
$\dot{\gamma}$	Strain Rate
$\dot{\gamma}_r$	Reference Strain Rate
Γ	Remoulding Coefficient
E	Erosion Rate

μ	Dynamic Viscosity
μ_{yield}	Bingham Viscosity
ν	Kinematic Viscosity
ξ	Turbulent Parameter
ρ	Material Bulk Density
σ	Total Stress
σ'	Effective Stress
τ	Shear Stress
τ_{yield}	Bingham Yield Stress
\bar{v}	Mean Velocity
φ	Dynamic Friction Angle
φ	Friction Angle
φ_i	Internal Friction Angle
φ_b	Bulk Friction Angle

Abbreviations

3D	Three Dimensional
AutoCAD	Automatic Computer Aided Design
ASCII	American Standard Code for Information Interchange
BGS	British Geological Survey
DAN3D	Dynamic Analysis 3D
DEM	Digital Elevation Model
DTM	Digital Terrain Model
GRD	Grid File Format
ISSMGE	International Society for Soil Mechanics and Geotechnical Engineering
NGI	Norges Geotekniske Institutt (Norwegian Geotechnical Institute)
SVV	Statens Vegvesen
UNESCO	United Nations Educational, Scientific and Cultural Organization

1. Introduction

The term “Landslide” refers to natural downwards movements which can contain a wide range of soil material. Rockfalls, rock slides, snow avalanches, quick clay slides, and debris flows are some of the few types of soil types or movements that the term “landslide” can refer to. Landslides can be devastating either for the urban infrastructures or/and by causing human losses.

There are several reasons which can be responsible for a landslide event. Geological formations, geotechnical properties as well as human intervention are the major causes of a landslide. The most common types of landslides in Norway are sensitive clay flows, snow avalanches and rock falls (Yifru 2014). There are more than 1000 human losses recorded only in Norway from landslides (Nigussie 2013). Recently, a new type of landslide is studied. Submarine landslides can be proved as catastrophic as the other types of landslides. They can cause serious damages, for instance, to the foundations of a bridge or they can even affect the coastline (Locat and Lee 2000).

The prediction or the prevention of a submarine landslide is a challenging task and a lot of uncertainties can occur. This is why extensive back-calculation analyses are required in order to minimize the uncertainties as much as possible. Mapping of the impacted areas and the prediction of the flow velocities and the thickness of the sliding mass are crucial elements concerning the risk reduction (McDougall and Hungr 2004). There are not many software programs or rheological models that describe the progression of a submarine landslide in precision. As a result, several alternatives

must be used, in order to make sure which the best way for a realistic regeneration of a submarine landslide is. For the present analyses, a quasi-3D code called DAN3D was used developed by (Hungri 2010). Both the analytical and empirical methods were used for the completion of this study and they are discussed in the subsequent chapters.

The examined submarine landslide exists south of Bergen, in Bjørnafjorden. A side-anchored floating bridge will be constructed, and the mooring system will be anchored on the seabed. The objective of the present study is the estimation of the governing parameters of the seafloor by conducting a series of back-calculation analyses. A post submarine landslide will be examined in order to understand the behavior and the progression of a submarine landslide event.

2. Description

2.1. General Background

The goal of the project E39 is to connect by road the city of Kristiansand with the city of Trondheim, passing through the west coast of southern Norway. The total length of the E39 is about 1100 km, it will reduce the travel time from about 22 hours to half. Statens Vegvesen (SVV), which is the contracting authority, is aiming to complete the project without having any ferry connections (Ferjefri E39). In the context of this goal, several bridges should be constructed in order to replace ferry connections. The present master thesis will be occupied with the construction of the bridge in Bjørnafjorden. This bridge will connect Os and Tysnes municipality in Hordaland County, located south of Bergen.

The planned bridge will have approximately 5 km length and the seafloor in that location is more than 500 meters beneath the sea level. Despite the different examined concepts and given the fact that the seafloor is too deep, two main options seem to distinguish. A curved end-anchored and a straight side-anchored floating bridge. Both bridges will have a suspended in their beginnings. However, the control of the lateral movement of the straight side anchored floating bridge is the main concern of the

engineering team. The adopted solution suggests the anchoring of the bridge on the seafloor in both sides of four of its pontoons across the bridge, which gives a total of 32 anchors. A successful and viable anchoring for the lifespan of the bridge is a very challenging task. The stability of the seafloor is the principal challenge that should be faced between several others.

The seabed of the fjord is mainly consisted of a main flat central basin being surrounded by steep flanks with slope angles which are often exceeding 30° . In the shallower areas, the terrain is mainly characterized by bedrock outcrops where no sedimentation was documented. Contrarily, there are several meters of sediments in the basin. There are three different types of anchors that will be used to rely on the seabed properties (seabed angle or sediment thickness). At the time being, the suggested anchors are gravity, suction and mixed (gravity and suction) anchors. Gravity anchors will be placed where there are almost no sediments. Suction anchors will be placed where the slope angle is more than 5 degrees with a clay layer more than 15 meters and mixed type anchors will be placed where the slope angle is more than 5 degrees with a clay layer from 5 up to 15 meters.

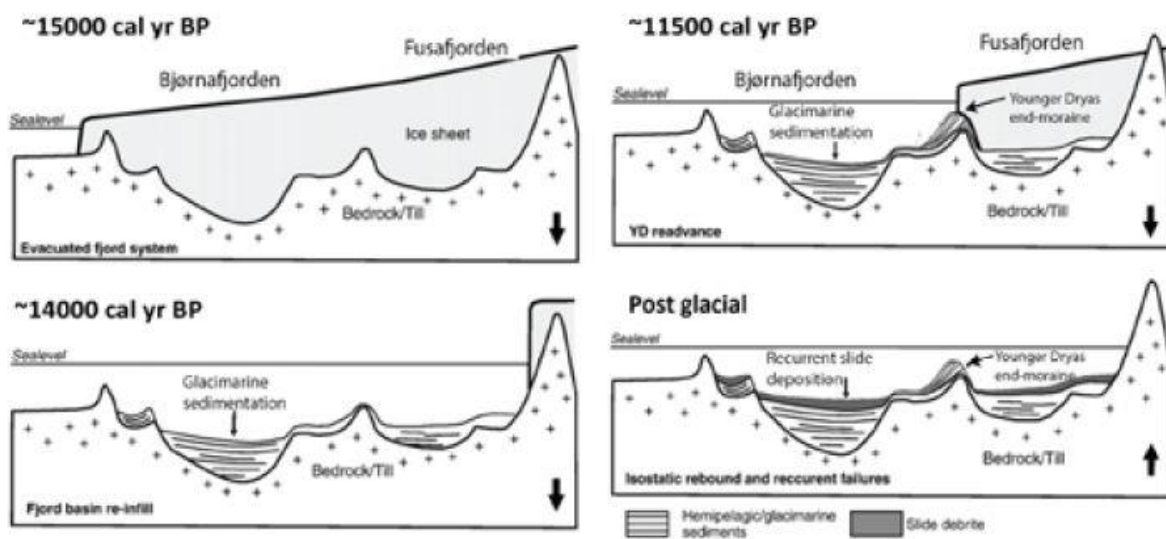


Figure 1: Simplified illustration of the glacial history in Bjørnafjorden, similar to all western Norwegian fjords. The sketch shows the maximum point of the glacier, glacimarine sediments' deposition, the progress of Younger Dryas and the mass deposits at the post-glacial period.

Most of the sediments are glacio-marine to hemipelagic clays. Glacial processes are mainly responsible for the soil conditions in the seabed of Bjørnafjorden. Deglaciation history took place in three phases (Figure 1). Before 15000 cal yr BP, the entire margin was covered from glaciers. The front part of the ice was quickly melted, resulting in some glacimarine sedimentation. At about 11500 cal yr BP the climate deterioration caused the recreation of the glaciers. The Younger Dryas lasted

approximately 1000 years. After the melting of the Younger Dryas (Mangerud 2000), moraines formulated a thick layer on the seabed (Kjennbakken, Mazhar et al. 2017).

Submarine instabilities as well as earthquakes, triggered in the past, can cause slope failures which will lead to debris flows. Every possible offshore infrastructure, like foundations, anchors or even communication cables, can be affected by debris flow. All possible instabilities must be examined and the impact of them must be evaluated. An analytic geohazard assessment of the slope stability of the seabed will provide valuable results of how vulnerable the anchor system to a debris flow can be and if the lateral support of the bridge is safe enough.

There is no efficient solution in which the seabed can be formulated in order to have acceptable factors of safety in every slope, next to the anchor places. As a result, the occurrence of a debris flow can be more than possible. The impact, which will have an incident like that, at the mooring system of the bridge must be examined and evaluated. For that purpose, a set of back-calculation analyses must be conducted in order to determine the governing magnitudes of a debris flow. Subsequently, many forward analyses must be conducted and the impact at the mooring system should be evaluated.

The geotechnical investigation which took place in Bjørnafjorden gave values for the required geotechnical parameters. For the analyses, the software DAN3D (Dynamic Analysis of Landslides in Three Dimensions) will be used, developed from professors Oldrich Hungr and Scott McDougall.

2.2. Main Objective

In Bjørnafjorden, several historical submarine slides are identified. In this site, a floating bridge anchored with mooring lines to foundations is proposed. Some of the foundations are located in places exposed to potentially unstable slope areas. It is thus important to study the impact of these potentially unstable masses on the nearby foundations. Back-calculation of submarine slides with various rheological models to establish parameters that govern the slide features such as run-out extent, velocity and possibly impact forces on foundations. The topography from Bjørnafjorden's seafloor was made available for this study in order to establish parameters which would be used in the numerical models.

2.3. Outline of the thesis

The present study has seven chapters, describing analytically of how it has been evolved.

Chapter 1: Introduction

Chapter 2: Description – in the second part some general background information is provided. Furthermore, a brief description of the studied area is given and how the geology of the area occurred together with the main objective of the study.

Chapter 3: Literature Review – is a part where some information about landslides together with their calcification is given. Different types of landslides (based on types of movements and included material) are discussed.

Chapter 4: Mathematical Background and Equations behind Rheological Models – in this part a description of the background of the used software is given. The governing mathematical expressions behind the rheological models, which have been used for the present study, are presented. This part gives a better understanding of how the rheological models simulate a given case and how the software deals with landslides from a mathematical perspective.

Chapter 5: Simulation Results of the Models – This is the part where all results of the study are presented. Moreover, it is described the procedure which was followed from the provided data until the final evaluation of the results. Empirical approach of the run-out distance and the methodology is also included. All results from the different rheological models are described together with their governing parameters. Furthermore, a description of the model that NGI used is given and a comparison between NGI study and the results of the present study is provided.

Chapter 6: Discussion of Results– The discussion part of the study includes all the comments for the results. The selected values of the parameters from the back-calculation of the landslide are given and the differences from the used and NGI's models are discussed. A comparison is also made among the two alternative promoted topographies. Finally, the actual landslide is compared with the simulation's results.

Chapter 7: Conclusions and Recommendations for Future Research – The final part includes conclusions which were occurred both from the results and from the comparison with NGI study. Finally, some recommendations and some suggestions for further investigation are given.

3. Literature Report

3.1. Introduction

Landslides is a complex phenomenon and sometimes an event that is difficult to be simulated. In the present chapter, description and classification of the different types of landslides is attempted based on the work of Polykretis (2013). It is a useful task contributing to the better simulation of a landslide event.

3.2. Definition

The term “landslide” has different definitions and theories over the years. The first definition was suggested by Terzaghi (1950). According to him, “*landslide refers to a rapid displacement of a mass of rock, residual soil, or sediments adjoining a slope, in which the center of gravity of the moving mass advances in a downward and outward direction*”. Subsequently, Zaruba and Mencl (1969) defined landslide as a rapid displacement of rocks due to a slide of a slope which is clearly separated

from a stable slope with a well-defined surface. Later, Coates (1977) established specific conditions for the classification of soil mass in landslides. These are:

- Gravity is a force that holds a principal role.
- The velocity of the movement must be relatively big.
- The movement can be denoted with different formats (falls, sliding or flow).
- The zone and the layer of the movement are not the same as a geological fault.
- The movement must follow a direction from downward and outward.
- The sliding mass must have defined boundaries and it is usually a limited part of a mountainous or hilly area.
- The sliding mass must include part of the mantle of the disintegration of rocks or/and part of the original rock.

Finally, Varnes (1978) used the term “*movement of mass*” in which is contained all movement of a slope due to sliding, fall, topple, flow and creep and he separated the definition of a landslide, sedimentation, and collapse. Varnes’ definition is the one which has predominated since nowadays.

Consequently, nowadays, with the broadest sense of the term, “*landslide*” is every change of the surface of a slope that comes along with the material’s movement with slow or sudden disturbance of its continuity. It constitutes a geological phenomenon that includes a wide range of mass movements of soils such as sliding, falls, topples and flows which can be met at main-land, coastal and wet environments (seas or lake). If a rock mass moves in a perpendicular direction, it is not called “*landslide*” but “*sedimentation*”, “*collapse*” or “*forfeiture*”. If the movement is along with a horizontal direction, then the general term “*landslide*” can be used.

3.3. Characteristics of Landslides

In 1978, Varnes, apart from the definition of the landslide, suggested a diagram (Figure 2) in which he illustrated the characteristics of an ideal landslide.

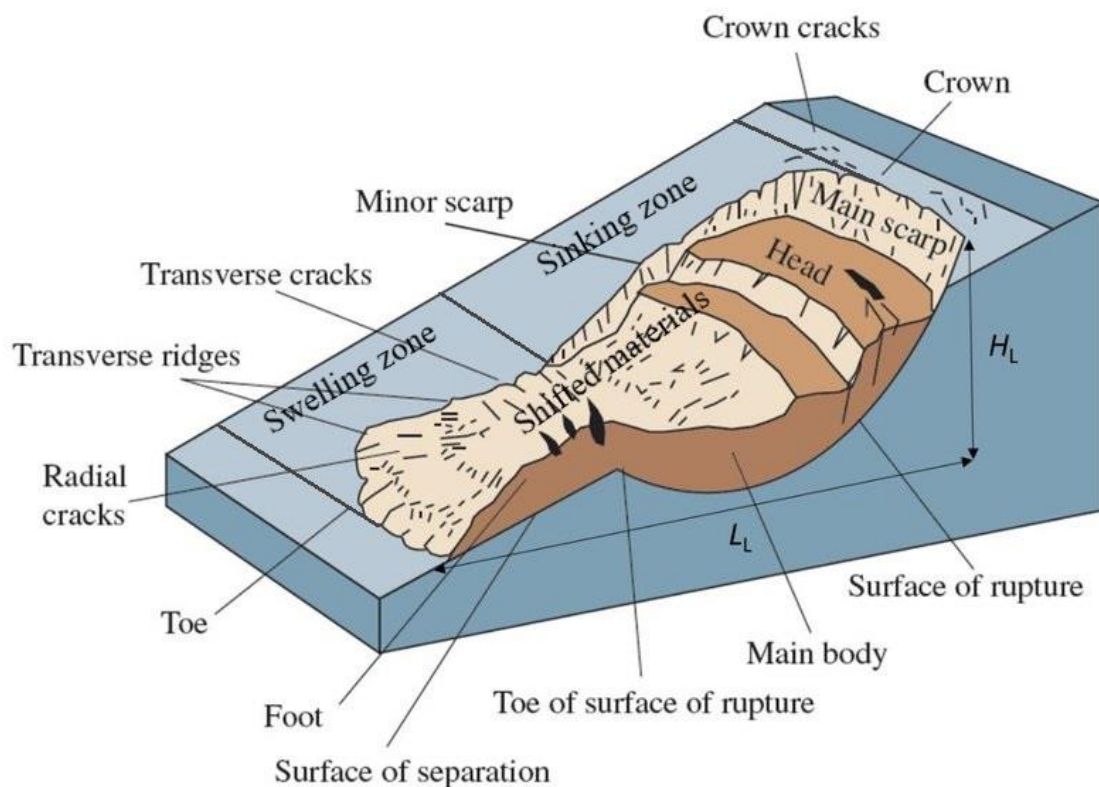


Figure 2: Graphical illustration of the main characteristics of an ideal landslide.

The main characteristics are presented as follows:

- **Main scarp:** is the main surface created in the undisturbed or immovable soil around from the surface of failure. It is caused due to sliding mass away from the undisturbed soil.
- **Secondary scarps:** are the sharp surfaces of the material which is moved and they are caused due to the internal differential movements of the sliding mass.
- **Head:** is located at the highest part of the landslide and it consists of the upper parts of the sliding mass along the main scarp.
- **Peak:** is the highest point of the head in the sliding mass which touches the main scarp.
- **Crown:** is the immovable soil which is located at the highest point of the main scarp.
- **Main body:** consists of the sliding mass of the material. It is shaped from the accumulation of the soil material. After the movement of the sliding mass along the path of the main scarp, the soil material is accumulated at the base of the main body of the landslide. In this point, the kinetic energy of the sliding mass zeros.

- **Surface of rupture:** is the surface on which the movement of the sliding mass takes place, due to the separation of the stable and undisturbed soil.
- **Surface of the separation:** is a part of the original terrain and it is covered from the toe of the landslide.
- **Foot:** is the lowest part of the main body.
- **Toe:** is the point of the sliding mass which is located the farthest from the main scarp.
- **Toe of surface of rapture:** is the cross section (usually buried) between the lowest limit of the surface of rapture and the original terrain.
- **Sinking zone:** consist the area of the landslide in which the sliding mass is located below the elevation of the original terrain.
- **Swelling zone:** is the area of the landslide in which the sliding mass is located above the elevation of the original terrain.
- **Minor scarp:** is the undisturbed soil material which is located on both sides of the surface of rapture. It can be described as “left” or “right” based on its relative position of the crown.
- **Shifted materials:** is the sliding mass which is displaced from its original position.
- **Original terrain:** is the surface of the slope before the event of the landslide.

3.4. Classification of landslides

Contrarily with other natural phenomena, the classification of landslides is a challenging task due to the fact that landslides are not perfectly recurring phenomena and usually are characterized from different causes, movements, morphologies, and types of materials. This is why, different scientific fields have suggested and developed a large number of classifications for the description of a landslide, which are based on various and different criteria. As a result, numerous different classification systems exist. According to Cruden and Varnes (1996), the main criteria are the type of movement, the type of the shifted material, activity and the velocity of the landslide, geology, morphology, climate and the geographical location of the landslide.

- **Type of movement:** is the main and the most significant criterion despite the uncertainties which can occur due to usually complicated motions. The main types are falls, sliding, flows but usually, movements such as topple, spread and complex movements are added as well.

- **Type of the shifted material:** Terms such as “*rocks*”, “*debris*” and “*earth*” are widely used for the separation of the materials which can be met into a landslide. For instance, the distinction among “*earth*” and “*debris*” is based on the percentage’s comparison of the material’s particles having a coarse grain size. If the percentage of the particles with a diameter larger of 2 mm is smaller than 20%, the material of the landslide is considered as “*earth*”, otherwise it is considered as “*debris*”.
- **Activity of the landslide:** is an important classification concerning the evaluation of future landslide events. This classification is based on UNESCO’s work (UNESCO 1993).
- **Velocity of the landslide:** is a parameter that can be related to the consequences of a landslide in urban infrastructures or by causing human losses. It can be characterized from extremely slow to extremely fast based on its average speed.
- **Age of the landslide:** The determination of a landslide’s age is an important issue concerning the risk assessment. An original landslide can be triggered again under specific natural circumstances such as earthquakes or intense rainfalls. It must be noted that landslides that happened in past geological years under specific environmental conditions, might be inactive (e.g. some alpine landslides which happened during Pleistocene are linked with specific tectonic, geomorphological and climatic conditions).
- **Geology:** is a significant factor of the morphological evolution of a slope.
- **Morphology:** Given the fact that the shifted material of a landslide is a geological volume with a “hidden side”, the morphological characteristics are extremely important in order to regenerate a technical assessment model.
- **Climate:** there is a special consideration at the climate condition because there is a possibility that contrasting climate conditions can lead to a different evolution of a landslide.
- **Geographical location of the landslide:** is a criterion describing the location of the landslides in a given area. As a result, several authors refer that they are occupied with a specific geographical-defined landslide like “*alpine landslides*”, “*landslides in plains*” or “*hilly landslides*”.

Nowadays, the British Geological Survey (BGS) follows the classification suggested by Varnes (1978) and Cruden and Varnes (1996). However, the terminology is based on the work of UNESCO (1990). This classification was one of the first and it combines the type of movement and the type of materials which are involved in. Figure 3 shows Varnes’ classification with a recent update suggested by Hungr, Leroueil et al. (2014)

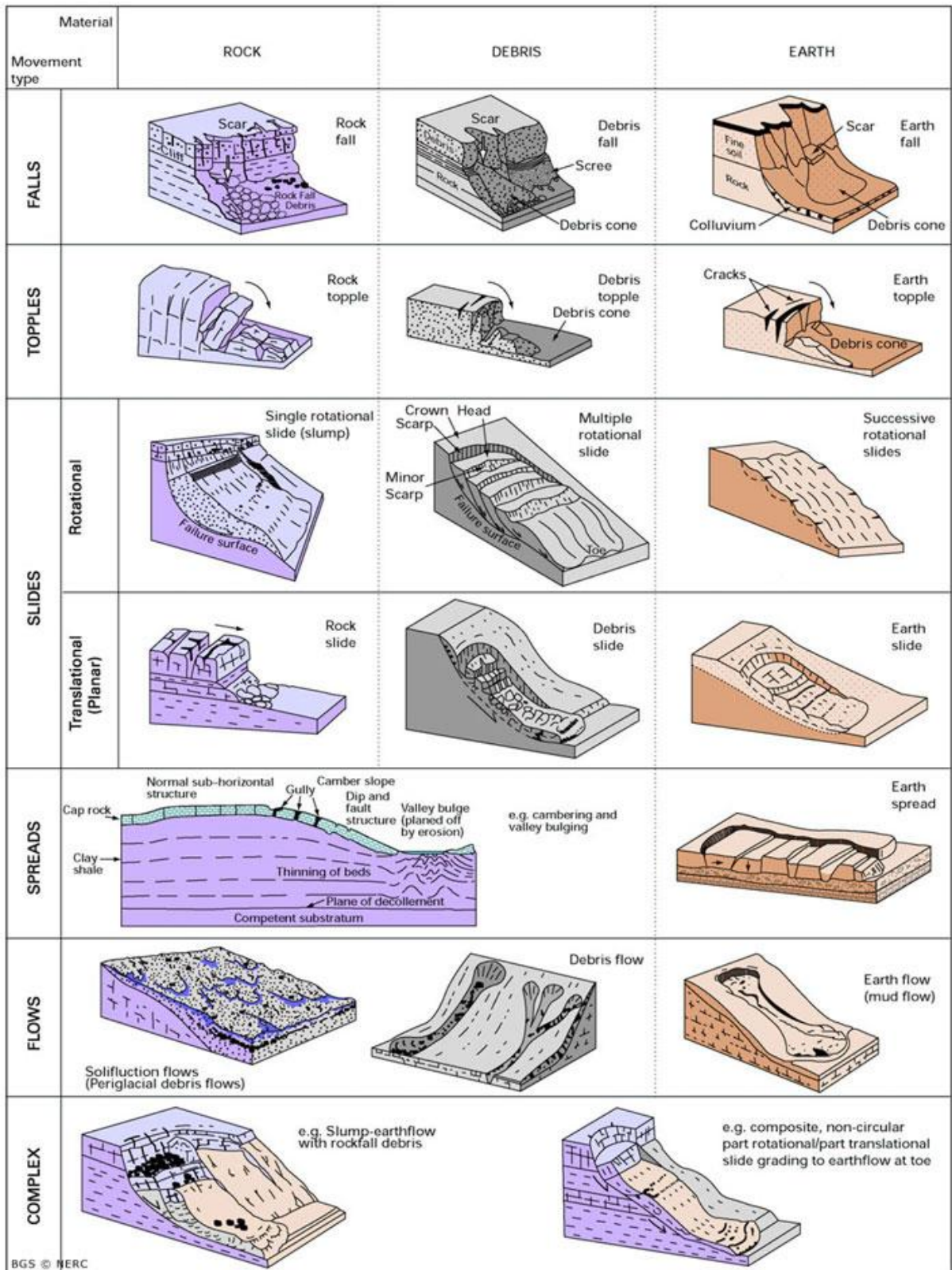


Figure 3: Classification according to Hungr, Leroueil et al. (2014). Landslides are separated based on the movement type and the material which is involved in it.

3.3.1. Falls

Falls can be described as mass movements of materials like earth or rocks which are detaching from steep slopes or cliffs along surfaces with little or no shear displacement. The detachment takes place along joints or fissures and the motion is through the air by free fall, bouncing or rolling. Falls can be extremely fast motions in terms of speed and they can be the result of smaller past movements. The main causes are the gravitational forces, differential erosion or excavations works.

3.3.2. Topples

Topples can be described as the forward rotation about a pivot point of rock, debris or earth masses. Subsequently, the movements can be modified to a fall or sliding based on the geometry of the slope, the type of the shifted mass and the surface of separation. The speed of topples motion can vary from slow to extremely fast and it is mainly met in rock slopes. Contrarily, debris and earth topples are very rare events and the occurrence of these is due to either natural processes or human interventions.

3.3.3. Slides

Slides are separated into “*Rotational*” or “*Translational*” slides based on the shape of the sliding surface. Rotational slides occur when masses slide outwards and downwards on one or more concave-upward failure surfaces that impart a backward tilt to the slipping mass, which sinks at the rear and heaves at the toe. The velocity of such movements can vary from extremely slow to extremely fast and the main cause is the overcoming of the shear strength of the material along the surface of rupture by the shear stress posed from the weight of the sliding mass.

Translational slides occur when movements slide along planar failure surfaces that may run, more or less parallel, to the slope. As the same with the rotational slides, the velocity can vary from extremely slow to extremely fast. Finally, translational rock slides are separated between a wedge and a planar failure based on the morphology of the slope.

3.3.4. Spreads

Spreads involve the fracturing and lateral extension of coherent rock or soil masses due to plastic flow or liquefaction of subjacent material. The presence of shear or tensile cracks facilitates the creation of spread landslides because they usually take place in smooth slopes or flat terrains. There are three types of spreads, “*Rock spreads*”, “*Liquefaction spreads*” and “*Complex spreads*”.

Rock spreads are observed when strong rock formation stands above weaker rock formation and vertical cracks separate the intact rock into smaller rock blocks. The underlying material is crushed and usually covers the created cracks. The displacement is spread through the body of the rock mass and the observed velocities are extremely slow.

On the other hand, liquefaction spreads are the soil failures caused by the process of liquefaction. Impregnated and loose sediments (usually sand layers) are transformed from a solid to a liquid state. After this, the upper cohesive materials (usually clays), which are supported on these liquified sediments, can be crushed and spread. Finally, cohesive material will be subsided, displaced, rotated, decomposed or liquified. Cracking is gradual but the spreads start suddenly without any warning sign and it is moving with high or slow speed. The main cause of the displacement can be either a short terrestrial or an artificial movement.

In the end, complex spreads consist of movements occurred as intense deformations of horizontal resistant and broken layers that cover cracked clays or soft shales

3.3.5. Flows

Flows are either slow or rapid movements of saturated or dry materials which advance by flowing like a viscous fluid and they usually follows an initial sliding movement. Some flows may be bounded by basal and marginal shear surfaces but the dominant movement of the displaced material is by the flowage. Rock, debris or earth flows are possible to occur. In rock flows, small deformations are observed that are distributed in ether small or bigger cracks but without any sign of displacement along a surface. They usually run in small distances.

On the other side, debris and earth flows are easily recognized as they run in bigger distances and they are intense due to the high cohesive material content. Debris flows are a fast mass movements in which a combination of uncompacted soil, rock, organic elements, air, and water is flowing in a downwards surface. Debris flows are mainly caused by the high-water flows due to extreme precipitation or the rapid snow melting which erodes and mobilize the loose material or the rock in

steep slopes. The resulting material can have a density of 2 ton/m^3 and a velocity of 14 m/s (Polykretis 2013). As a result, a debris flow can carry trees, cars or even houses away, exclude bridges or cause floods in areas along its path. Debris flow can be easily confused with a normal flood, but they are two different procedures. Earth-flow is either a slow or a rapid movement, consisted of fine materials or clay rocks. The flow is elongated and stands out from the debris flow due to its shape which is similar to an hourglass.

Finally, if flows have extremely slow velocities, they are classified as creep. Creep is indiscernible rather than stable and downwards mass movement. There are three categories of creep, seasonal, continuum and progressive. Seasonal creep is influenced by seasonal variations such as humidity and soil temperature. Continuum creep occurs when the shear pressure continuously exceeds the strength of the material. Finally, progressive creep occurs when a slope reaches a failure point as another mass movement type.

3.3.6. Complex

Complex movements are the result of the combination of two or more movements that have already described above. They are occurred either in different parts of the sliding mass or in different stages of the movement evolution.

3.5. Submarine Landslides

The developing of the oil and gas industry, and the need for transport and communication, both surficial and beneath the sea level, led the scientists to study the stability of seafloor. Movements of submarine soil masses can lead to serious damages at the coastline or in urban infrastructures. The causes of a submarine landslide can be various and not necessarily unique. During the years many researchers pointed different causes of a submarine landslide. According to Locat and Lee (2000) some of them can be:

- Over-Steepening
- Seismic Loading
- Storm-Wave Loading
- Rapid Accumulation and Under-Consolidation

- Gas Charging
- Gas Hydrate Disassociation
- Low Tides
- Seepage
- Glacial Loading or
- Volcanic Island Processes

Submarine landslides can be studied from a geotechnical scope (Leroueil, Locat et al. 1996). However, the complexity of them is great and it is not obvious that submarine landslides develop only in one phase (Norem H. 1990). An illustration of the evolution of a submarine landslide is graphically represented from Meunier (1993) (Figure 4). Consequently, in a submarine landslide, different principles are applied. Soil and rock mechanics, fluid mechanics or torrential hydraulics principals can have an application on the study of a submarine landslide (Locat and Lee 2000). According to ISSMGE (International Society for Soil Mechanics and Geotechnical Engineering), submarine landslides can be classified under the category of flows. However, there is a fundamental difference with all the other type of flows. Submarine landslides can develop turbidity currents that cannot be developed in avalanches, debris, and mud-flows (Locat and Lee 2000).

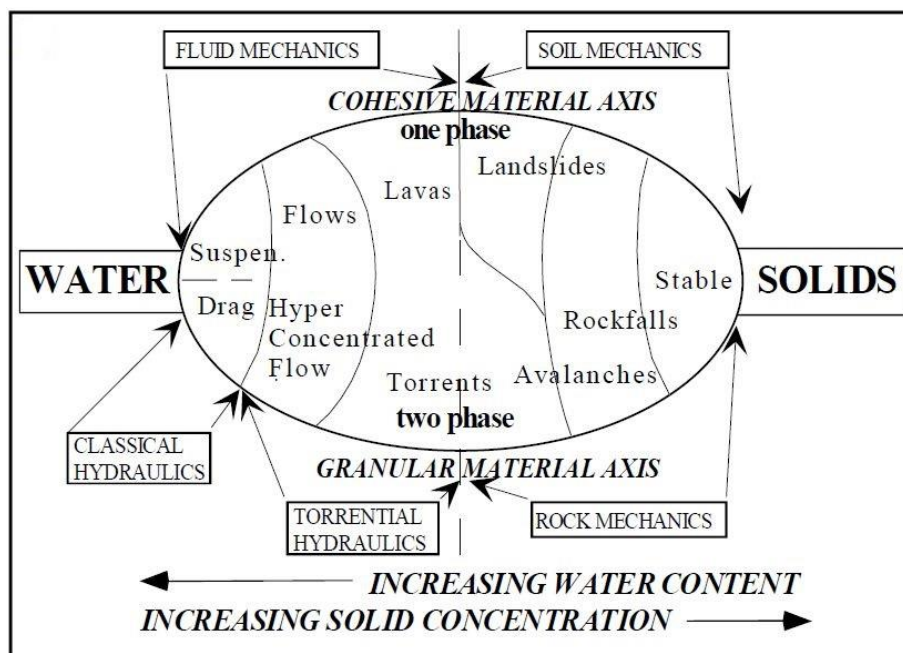


Figure 4: Graphical illustration of mass movements made of solid and water mixtures at various stages of mixing proposed by Meunier (1993).

4. Mathematical Background and Equations behind Rheological Models

4.1. DAN3D Model

The chosen software for running the analyses is DAN3D (Dynamic Analysis of Landslides in Three Dimensions), which is a Windows-based software. DAN3D is suitable for the prediction of the movement and the velocity of a rapid developing landslide. There are different types of landslides like avalanches and debris flows, rock avalanches and flow slides. This software is tested for several landslides but there is a lack of studies on quick clay landslides (Thakur, Nigussie et al. 2014). This software is a useful tool for the estimation of the run-out evolution based on data that can be provided by the software user (Hungr 2010). An analytic description of DAN3D can be found in Hungr (1995), McDougall and Hungr (2004) and (McDougall and Hungr 2005).

The approach of this software is semi-empirical, and it is based on the simplified concept of “*equivalent fluid*” (Hungr and McDougall 2007) (Figure 5). DAN3D was specifically designed to give a practical simulation of landslides by inputting parameters’ values which came up from the back-

calculation of historical cases. The aim of DAN3D is to provide simple solutions from a small number of inputted parameters and take into account some important aspects of a landslide movement. Different rheologies, heterogeneity, internal stiffness and the ability to entrain material from the path (S. and Hungr 2003).

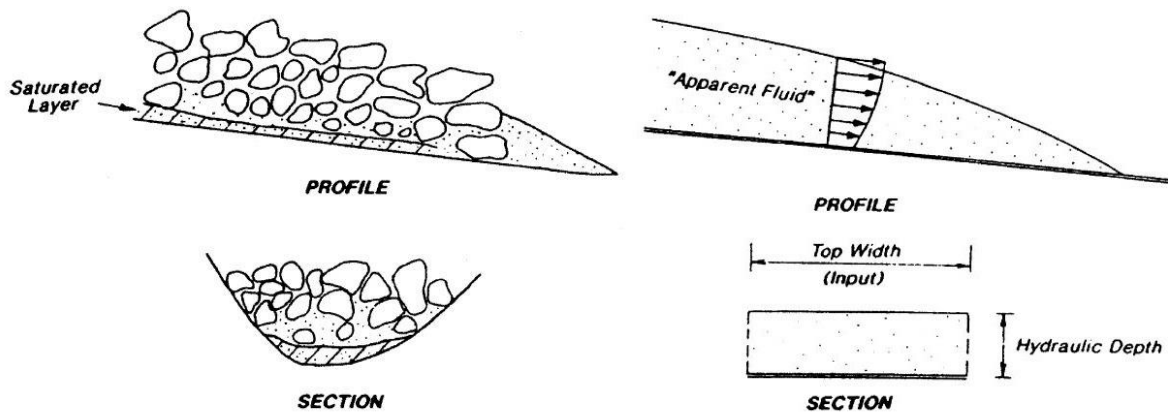


Figure 5: Illustration of the semi-empirical approach of "Equivalent Fluid".

4.2. Concept of "Equivalent Fluid"

In contrast with fluids, landslides can be proved complex and difficult to be studied. The reason for this is that landslides do not follow the known assumptions of isotropic internal stresses, hydrostatic and homogeneity of the material. Furthermore, materials included in landslide can follow non-Newtonian rheologies which can make the study of a landslide an even more complex and challenging task. Given the complexity of such a phenomenon, it is almost impossible to apply a single relationship that can govern a landslide. Consequently, the traditional approach cannot be implemented.

DAN3D adopted the concept of "Equivalent Fluid" which is a semi-empirical approach, introduced by Hungr (1995). In the context of this concept, a complex landslide is modeled as a homogenous material, which is governed from simpler rheological expressions. However, the internal and the basal rheology can vary, and they can follow different equations. The main idea of this has roots of how classical fluid dynamics are faced. The basal rheology is governed from viscous or turbulent expressions and the main body of the fluid is considered to be hydrostatic. Additionally, this idea is also supported by the literature (Savage and Hutter 1989) and (Pudasaini and Hutter 2007) and what they named as SH model. The basal and the internal rheology of that model are frictional but with different friction coefficients. It is a model used for the simulation of sand flows or avalanches with a

weak frictional basal layer (Hung and McDougall 2007). DAN3D is based on this idea of the SH model. The main difference is the replacing of the basal friction rheology and providing the user the option of choosing between different rheologies.

Both the SH model and the DAN3D are considered that the internal rheology is frictional. Consequently, the internal friction angle (ϕ_i) is the only governing parameter. If the internal friction angle is equal to zero, the model is similar to hydrostatic stress distribution. On the other side, the basal rheology is generally governed from couple parameters which can be easily determined from a back-calculation of a landslide. The values of the parameters from such calculation can be judged based on the final result of the landslide in terms of how realistically the regeneration of the original landslide is. Therefore, the values of the parameters can vary from those which had been determined in the laboratory. An extensive back-calculation of a landslide is needed for the determination of these parameters resulting in a reduced dependency from laboratory results. However, given the simplicity of those rheological models and the limited number of input parameters a careful choice of a rheological model has to be made. For instance, if a frictional rheological model is chosen, high relative velocities can be produced. However, a Voellmy rheological model produces lower velocities and deposits that bugle forward.

Voight and Pariseau (1978) underline that: “*Any model that allows the slide mass to move from its place of origin to its resting place in the time limits that bound the slide motion is likely to be consistent with the principal observable fact—that of the slide occurrence itself*”. Following the previously employed logic, any continuum dynamic model which can be regenerated by the evolution of a landslide within a given time and deposition can be considered useful, no matter what the governing microscale mechanisms are,.

Finally, the back-calculation of a landslide cannot be based only in one simulation. A very usual wrong argument is that only one set of parameters can correctly predict the evolution and the behavior of a specific landslide event. In every case, different sets of parameters should be proposed which can describe the same event.

4.3. Governing Equations

DAN3D is based on Lagrangian expressions of the depth-integrated St. Venant equations, applied in curvilinear coordinates. An analytic derivation of those expressions is provided in the Ph.D. thesis by McDougall (2006). DAN3D starts with the equation governing the mechanics of continuum (Equations 1 & 2).

$$\frac{\partial \rho}{\partial t} + \nabla * \rho v = 0 \quad (1)$$

$$\frac{\partial(\rho v)}{\partial t} + \nabla * \rho v \otimes v = -\nabla * T + \rho g \quad (2)$$

where ρ is the material bulk density, t is the time, v is the velocity vector, T the stress tensor, g the gravitational acceleration, ∇ the gradient operator, $*$ represents the dot product and \otimes denotes the tensor product.

This general form of Equations (1), (2) can be simplified by introducing three main logical assumptions:

1. The material of the landslide is assumed to be incompressible and has constant density.
2. All boundary conditions should be applied.
3. A conversion to a Lagrangian coordinate system must be done.

The first assumption seems logical since granular materials have small density variations especially compared with other dynamic variables (Savage and Hutter 1991), (Brufau, Garcia-Navarro et al. 2000), (Denlinger and Iverson 2004). The boundary conditions together with the depth averaging can be applied based on Leibniz's rule. The top surface of the flow has zero stress, and this is the first condition. At the basal layer, the chosen rheological expression controls the stress tensor which is consisted of normal stress and it corresponds to the hydrostatic potential and a shear-resisting motion. Furthermore, the material entrainment is taken into account by letting the volume fluxes across the layer at the base. However, plowing is a phenomenon that applies to a free surface and it can occur at the front part of the flow. DAN3D considers plowing as an erosion component of the basal layer. The term "Erosion Rate" (E) is the rate at which the material is located at the bottom entrance to the main body of the landslide (Takahashi 1991) and the values of the erosion rate must be positive (Hung and McDougall 2007). The last assumption is the introduction of a Lagrangian coordinates system. In DAN3D the z -direction follows the bed-normal direction and the x -direction follows the movement of the landslide (Figure 6). Applying all the assumptions to the continuity equation is (Equation 3):

$$\frac{Dh}{Dt} + h \left(\frac{\partial(v_x)}{\partial x} + \frac{\partial(v_y)}{\partial y} \right) = E \quad (3)$$

where ρ is the density, v is the mean velocity and g is the gravity acceleration in x-, y-, and z-direction.

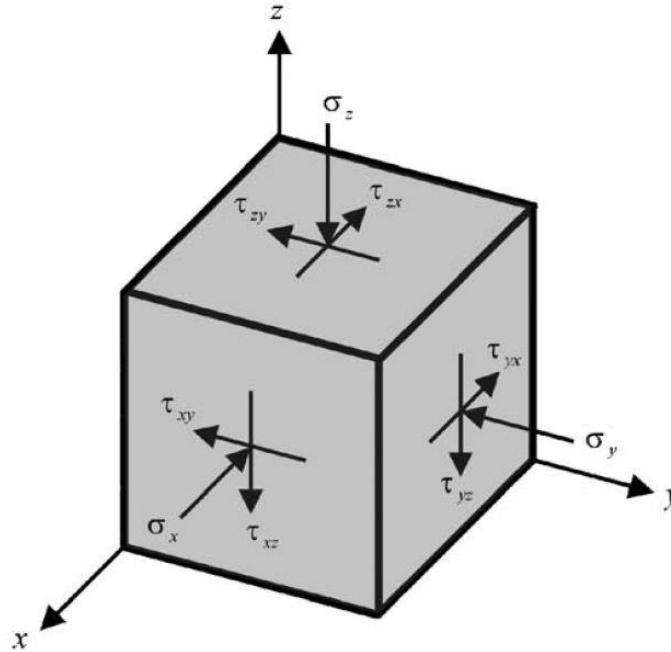


Figure 6: Total Stresses situation on a landslide's material particle. They are also visible in the directions of z- and x-axes.

There are two main reasons, why the Lagrangian approach is convenient. First of all, the momentum balance equations do not contain any term with acceleration. As a result, numerical integration is easier. Secondly, a more accurate approach can be achieved, given the fact that the computational resources can be gathered into the mass of the landslide. Additionally, another advantage of the Lagrangian approach can be the simpler way that the path curvature is being faced, especially compared with the Eulerian approach. The transformation of Lagrangian forms after the depth averaging is shown below (Equations 4, 5 & 6).

$$\rho h \frac{Dv_x}{Dt} = -\frac{\partial(\sigma_x h)}{\partial x} - \frac{\partial(\sigma_y h)}{\partial y} + \tau_{zx} + \rho h g_x - \rho v_x E \quad (4)$$

$$\rho h \frac{Dv_y}{Dt} = -\frac{\partial(\tau_{xy} h)}{\partial x} - \frac{\partial(\sigma_y h)}{\partial y} + \rho h g_y \quad (5)$$

$$\rho h \frac{Dv_z}{Dt} = -\frac{\partial(\tau_{xz} h)}{\partial x} - \frac{\partial(\tau_{yz} h)}{\partial y} + \sigma_z + \rho h g_z \quad (6)$$

Moreover, if it is considered that the depth is not constant, and it is small compared with the length and the width of a landslide, the terms of τ_{xz} and τ_{yz} are relatively small compared with the basal total bed-normal stress σ_z . Consequently, they can be neglected.

The Lagrangian derivative v_x is equal to the acceleration of the motion while the mass is moving in the x-direction (Equation 7) because the axes are aligned with the movement of the landslide.

$$\frac{Dv_z}{Dt} = \frac{v_x^2}{R} \quad (7)$$

where R is the bed-normal curvature radius in the direction where the landslide moves.

In the z-direction, with an inclination of α degrees, the gravity is (Equation8):

$$g_z = -g \cos \alpha \quad (8)$$

Consequently, if all the expressions above are combined, the bed-normal basal stress is (Equation 9):

$$\sigma_z = \rho h \left(g \cos \alpha + \frac{v_x^2}{R} \right) \quad (9)$$

Some last simplifications can be succeeded with the consideration of the classical soil mechanics theory. According to Terzaghi and Peck (1967), all stresses increase linearly with depth. Therefore, it is possible that stresses by using pressure coefficient (k) (Equations 10 & 11). The fact that the normalization is conducted on total stresses and not on effective stresses is detailed described on Hungr and McDougall (2007) (Figure 7).

$$\sigma_x = k_x \sigma_z \quad (10)$$

$$\tau_{yx} = k_{yx} \sigma_z \quad (11)$$

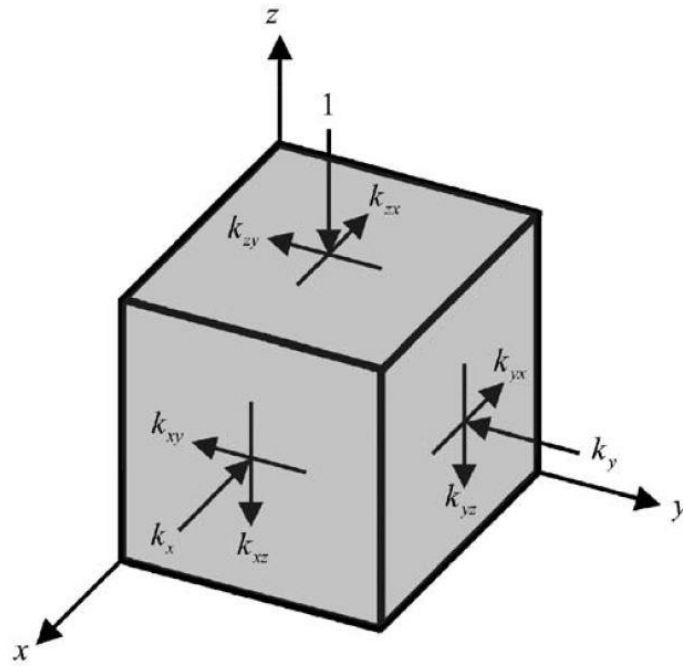


Figure 7: Normalizing coefficients on total stress situation on a landslide's material particle. Stress coefficients are considered positive.

The final assumption is the neglect of the spatial variation in the context of the normalized stress state because they are small. As a result, by neglecting relatively small terms and rearranging the terms of the Lagrangian forms, which are averaging the depth in the x- and y-directions, the final formation is as follows (Equations 12 & 13).

$$\rho h \frac{\mathbf{D}v_x}{\mathbf{D}t} = \rho h g_x - k_x \sigma_z \frac{\partial h}{\partial x} - k_{yx} \sigma_z \frac{\partial h}{\partial y} + \tau_{zx} - \rho v_x E \quad (12)$$

$$\rho h \frac{\mathbf{D}v_y}{\mathbf{D}t} = \rho h g_y - k_y \sigma_z \frac{\partial h}{\partial y} - k_{yx} \sigma_z \frac{\partial h}{\partial x} \quad (13)$$

where \mathbf{D}/\mathbf{D} symbolizes the Lagrangian differential operator.

The left part of both equations can be derived with the consideration of the dynamic equilibrium. The first component of the right side is the gravity force term. The next two are the pressure components, the fourth term is the shear stress which resists on the basal motion and the fifth term takes into account the momentum flux because of the material which entrains to the mass of the landslide.

4.4. Basal Rheological Models

The internal rheology of the material is considered to be frictional and the governing parameter is the internal friction angle (φ_i). Contrarily, the rheology on the base can vary between several rheological models. The shear stress at the base (τ_{xz}) resists to the movement of the landslide. As a result, it is negative, according to the reference coordinate system which has been chosen. Following the concept of “*Equivalent Fluid*”, the basal rheology expression can be different from the internal rheology. In order to simulate different types of landslides, several options of rheological models are provided. The user can choose between Frictional, Plastic, Newtonian, Bingham and Voellmy rheologies. The governing equations (τ_{xz}) of every rheological model are listed below. For a detailed description of the equations and the numerical solution methods, the Ph.D. thesis of McDougall (2006) is proposed.

At the **Frictional rheology**, the basal shear stress (τ_{xz}) is directly depended to the basal effective stress σ'_z (Equation 14).

$$\tau_{xz} = -(\sigma_z - u) \tan \varphi = -\sigma'_z \tan \varphi \quad (14)$$

where φ is the dynamic friction angle at the basal layer.

The determination of the pore pressure (u) is a very challenging, if not impossible, task in a dynamic event such as a landslide. This is due to the continuous change of the total normal stress and the existed time-dependent diffusion. As a result, instead of pore pressure, the pore-pressure coefficient ($Ru = u/\sigma_z$) is used. Equation 14 is transformed as follows (Equation 15).

$$\tau_{xz} = -\sigma_z(1 - r_u) \tan \varphi \quad (15)$$

The assumption that the pore-pressure coefficient (Ru) is remaining constant during the event of a landslide, leads to the conclusion that Equation 15 remains proportional. Further simplifications can be applied if the bulk friction angle (φ_b) ($\varphi_b = (1 - r_u) \tan \varphi$) is introduced at the basal layer. The final format of the expression is shown below (Equation 16).

$$\tau_{xz} = -\sigma_z \tan \varphi_b \quad (16)$$

Plastic rheology is related to a pseudo-static analysis that can simulate the motion of liquified debris. The basal shear stress (τ_{zx}) is assumed to be equal to shear strength (Equation 17).

$$\tau_{xz} = -c \quad (17)$$

Newtonian rheology is useful in the case of a landslide which is fully liquified. It can also contain granular or clayey materials. The governing basal shear stress τ_{zx} equation is (Equation 18):

$$\tau_{xz} = \frac{3\mu v_x}{h} \quad (18)$$

where μ is the dynamic viscosity.

Bingham rheology is a combination of plastic and viscous flow behavior. The dual behavior of a so-called Bingham fluid is related to the yield strength. Below the threshold yield strength, the material behaves as a rigid but it as a viscous material above. The basal shear stress (τ_{zx}) is the solution of the cubic equation below (Equation 19):

$$\tau_{zx}^3 + 3\left(\frac{\tau_{yield}}{2} + \frac{\mu_{Bingham} v_x}{h}\right)\tau_{zx}^2 - \frac{\tau_{yield}^3}{2} = 0 \quad (19)$$

where τ_{yield} is the Bingham yield stress and $\mu_{Bingham}$ is the Bingham viscosity.

Voellmy rheology is mostly used for the simulation of snow avalanches (Thakur, Nigussie et al. 2014). The basal shear stress (τ_{zx}) equation (Equation 20) contains two parameters which are combining both the frictional and the turbulent behavior.

$$\tau_{xz} = -\left(\sigma_z f + \frac{\rho g v_x^2}{\xi}\right) \quad (20)$$

where f is the friction coefficient as the same with the Equation (14) and ζ is a turbulent parameter, firstly introduced by Voellmy (1955), which is analogous to the square of the Chézy coefficient (Hungr and McDougall 2007).

5. Simulation Results of the Models

5.1. Introduction

All simulations were conducted with DAN3D and will be presented in this chapter. The examined landslide located in Bjørnafjorden, south of Bergen. A multilevel analysis was conducted, and it will be presented as follows:

- Empirical Calculation of the Run-Out Distance.
- Numerical Approach with Different Rheological Models.
- Comparison with NGI Results.

The first level of the analysis is an empirical approach of the run-out distance. A literature study was made, and several empirical expressions used for the estimation of the run-out distance. The major challenge at that point of the study was the finding of a suitable expression for submarine landslides. Even though no empirical expressions, concerning submarine landslides, were found, some realistic approaches were made, with other expressions mainly developed for debris flows.

The next level of the analysis part is the numerical back-calculation of the landslide. It was necessary that the topography had to be modified. The way that DAN3D is built requires a careful estimation of the topography before the given landslide happens. Two different topographies were promoted and for that purpose, both were tested in order to be clarified which one simulates the landslide more realistically. For the simulation two rheological models were used. Initially, a more simple and compatible with the known parameters, the rheological model was chosen (Plastic Material Type). A set of parameters was selected based on the quality of the results from this model. In parallel, the topography which simulated better the landslide was chosen for further study. It was deemed necessary that a second rheological model should be used. Consequently, the frictional rheological model was selected (Frictional Material Type) for a series of reasons which are analytically presented at the next sub-chapters. Both rheological models are compared and discussed in the next chapter.

The third part is a comparison between the NGI analysis and the present study. NGI have already back-calculated this submarine landslide by using different rheological models. A two-leveled comparison was made. Firstly the results of the present with NGI's study are compared and secondly, the proposed parameters from NGI were used in order to run analyses. Consequently, an evaluation of how the proposed parameters from NGI behave in different rheological models. NGI exclusively used the Hershel-Bulkley rheological model. Unfortunately, DAN3D does not include Hershel-Bulkley rheological model and therefore not all of the required parameters, of each rheological model, were matching. Consequently, only the matching parameters were used and the others were neglected.

5.2. Empirical Approach

The calculation of a run-out distance is one of the main tasks when studying a landslide. There are both analytical and empirical ways to calculate a run-out distance. Many software programs (DAN3D, RAMMS, BING3, RASH3D, FLO2D, etc.) are used to estimate the progression of a landslide. As a result, a more accurate calculation of a run-out distance can be done (Hungr and McDougall 2007). However, an empirical approach is useful and a very good indicator as well. Especially at the beginning of a study, the empirical approach is the most common way to calculate the major results.

For the present master thesis, literature research was conducted and several empirical methods were found which were useful to predict the run-out of different types of landslides. The major problem was that the studied landslide is submarine and there were not empirical relationships for that case. Consequently, different relationships were tested in order to clarify if the results could be correlated with the actual run-out distance. According to Zhan, Fan et al. (2017) a general format for such an equation could have a format (Equation 21):

$$L = C1 * V^{C2} \quad (21)$$

where L is the run-out distance, V the volume of the sliding mass and C1 and C2 constants.

However, other researchers (Qarinur 2015) suggest a similar format (Equation 22):

$$L = C1 * H^{C2} \quad (22)$$

where L is the run-out distance, H the height as shown in Figure 8 and C1 and C2 constants, the values of which can vary depending on the type of the examined landslide.

The studied landslide was a run-out distance (L) about 510 m resulted from a volume (V) of approximately 170000 m³ and a height (H) around 96 meters.

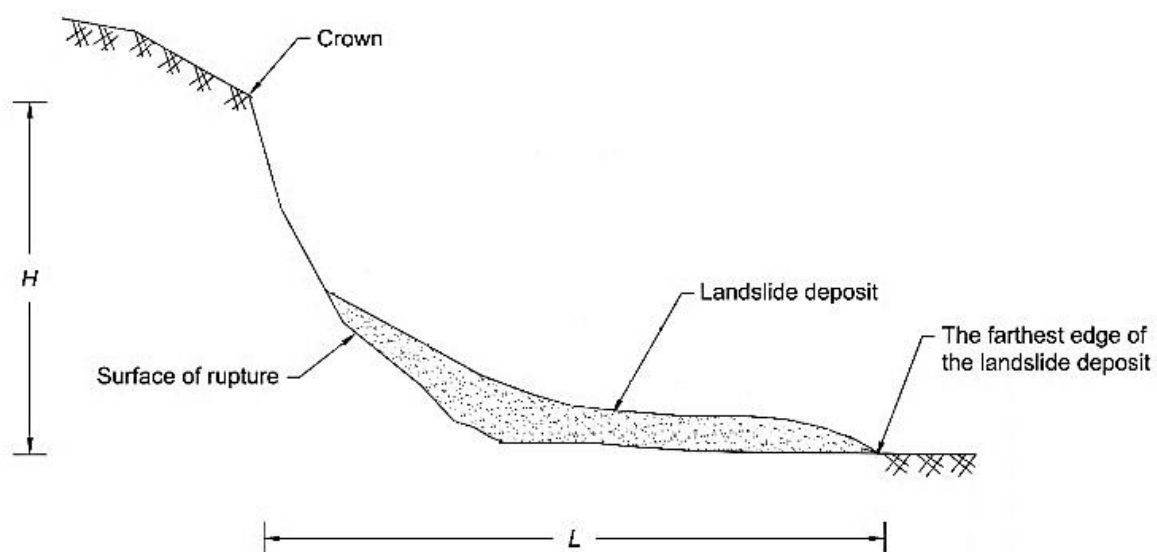


Figure 8: Typical section shows the Height (H) and the Length (L) of a debris flow. Both height and length are measured from the crown until the farthest edge of the landslide's deposit in the vertical and horizontal directions respectively.

Qarinur (2015) suggests different expressions while he is correlating different parameters. For every expression, a coefficient of determination (R^2) is given showing that the correlation between the different parameters is acceptable. The coefficient of determination is interpreted as the proportion of the variance in the dependent variable that is predictable from the independent variable. Debris flows

are complex phenomena and they may not be dependent only in one parameter. Values close to 1 confirm the direct dependency of two different parameters.

Furthermore, some limit expressions are provided. L_{max} and L_{min} are the maximum and the minimum run-out distances (m), respectively. As a result, it can be identified if the run-out distance is within the proposed limits. In order to have an optical overview of how close every approach is, a graphical representation is given.

A general expression (Equation 23) for all different types of landslides, such as debris flows as well as for rotational or translational slides and rock falls, which is proposed by Qarinur (2015), is showing below together with the limit expressions (Equations 24 & 25). The coefficient of determination (R^2) is 0.79. The height of the slope should be within the range from 4 to 220 meters (Qarinur 2015).

$$L = 1.066 * H^{1.093} \quad (23)$$

$$L_{min} = 0.364 * H^{1.093} \quad (24)$$

$$L_{max} = 3.138 * H^{1.093} \quad (25)$$

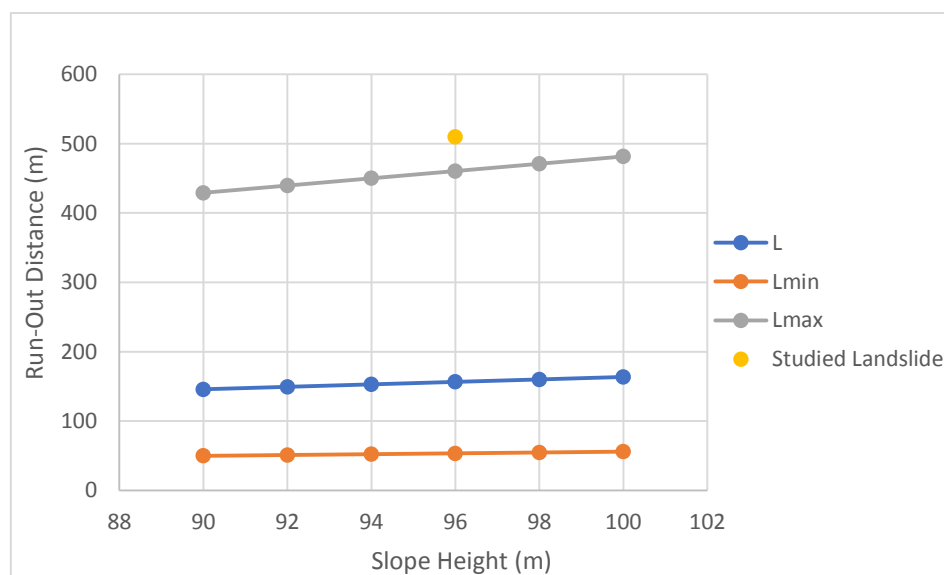


Figure 9: Graphical illustration of the approach of the empirical expression which can be used for debris flows, rotational or translational slides and rock falls.

It seems (Figure 9) that the equations cannot correctly predict the run-out distance of the original landslide, even if it is close to the upper limit. Consequently, other approaches should be examined.

The second approach (Equations 26, 27 & 28) was developed only for debris flows. The coefficient of determination (R^2) is 0.54 and the height range should be within 17 and 185 meters (Qarinur 2015).

$$L = 0.982 * H^{1.290} \quad (26)$$

$$L_{min} = 0.233 * H^{1.290} \quad (27)$$

$$L_{max} = 3.378 * H^{1.290} \quad (28)$$

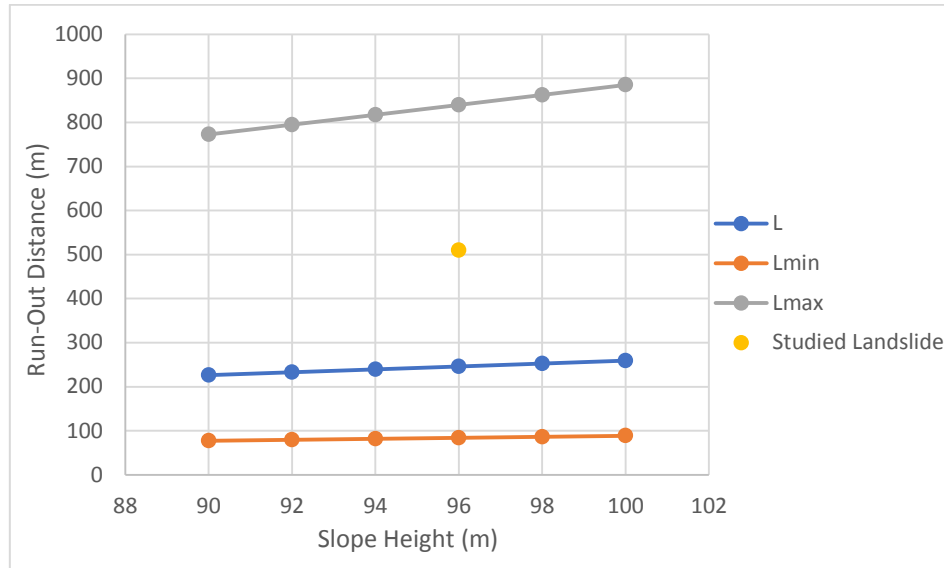


Figure 10: Graphical illustration of the approach of an empirical equation developed for debris flows.

The fact that the coefficient of determination is not close to 1 confirms the dependency of this phenomenon is not only based on the slope's height but also on several parameters. This can also be obvious from the wide range among the limit equations (Figure 10). Consequently, even if the studied case is within the acceptable range other approaches, which can be more accurate, should be considered.

A more accurate expression for the prediction of the run-out distance could come of taking into account the cause the landslide. In Bjørnafjorden the most common cause of landslides is earthquakes which happened a few thousand years ago (NGI 2017). An empirical approach (Qarinur 2015) for landladies triggered by earthquakes is described by the Equations (29), (30) and (31). The coefficient of determination (R^2) is 0.81 and the slope heights can vary from a minimum of 10 to a maximum of 185 meters (Qarinur 2015).

$$L = 0.574 * H^{1.380} \quad (29)$$

$$L_{min} = 0.233 * H^{1.380} \quad (30)$$

$$L_{max} = 1.520 * H^{1.380} \quad (31)$$

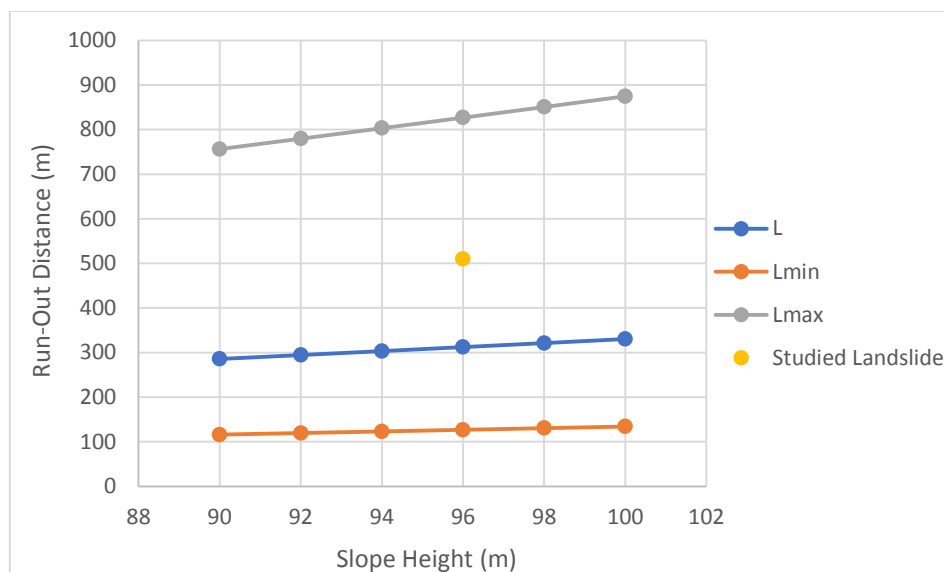


Figure 11: Graphical illustration of the approach of an empirical equation developed for landslides caused by earthquakes.

The approach (Figure 11) is better than it was in the previous approach (Figure 10) but the difference among the studied landslide and the empirical approach is still big.

An estimation coming of the correlation between the volume of a debris flow and the run-out distance was studied. For that case, two different average approaches were found. Equations (32), (34) and (35) are suggested by Qarinur (2015) and Equation (33) by (Zhan, Fan et al. 2017). The coefficient of determination (R^2) is 0.79 and 0.83 respectively and the scale of the debris flow can vary from a very small to an enormous one (Qarinur 2015) (Zhan, Fan et al. 2017).

$$L_1 = 1.131 * V^{0.474} \quad (32)$$

$$L_2 = 4.519 * V^{0.377} \quad (33)$$

$$L_{min} = 0.337 * V^{0.474} \quad (34)$$

$$L_{max} = 3.799 * V^{0.474} \quad (35)$$

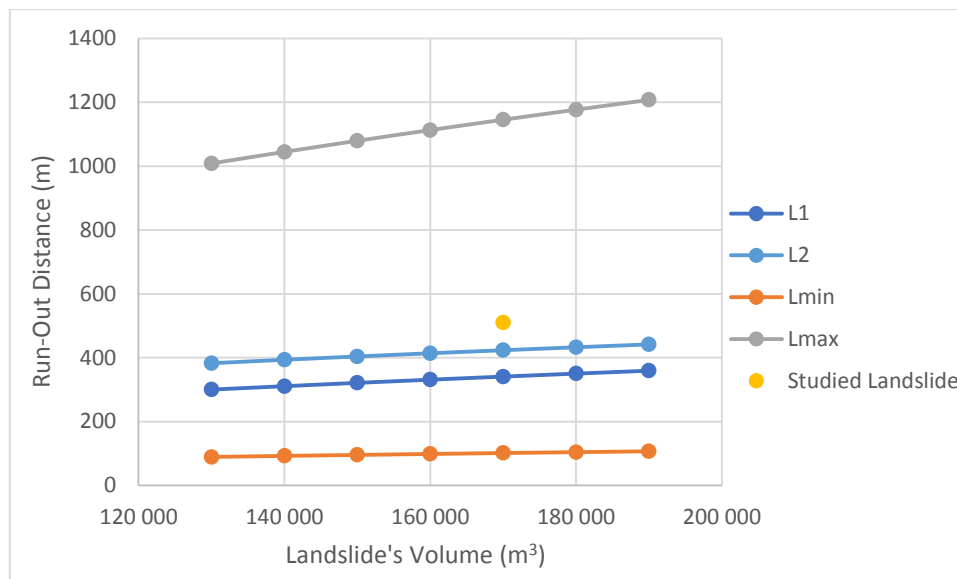


Figure 12: Graphical illustration of the approach of an empirical equation developed for debris flows. The run-out distance is calculated based on the sliding mass' volume.

Expressions (32) and (33) approach the run-out distance of the examined landslide very well. It seems that the last correlation is the most accurate, and it can predict better the run-out distance.

The final approach has been made with the proposed expression from Rickenmann (1999). This approach is a combination of volume and the height of the landslide (Equation 36). This expression came up from an extensive study of 154 debris flow events worldwide (Nigussie 2013).

$$L = 1.9 * V^{0.16} * H^{0.83} \quad (36)$$

Using this final approach and given the parameters of the examined landslide (Volume = 170000 m³ and Slope Height = 96 meters), the calculation of the run-out distance is slightly overestimated (around 577 meters) but it is not far away from the actual distance. The graphical illustration of this approach seems to be difficult. Given the number of the governing parameters, the graph should be in three dimensions, and the usefulness of it, would not be significant since only one point needs to be compared.

5.3. Procedure for Simulations using DAN3D Models

All the provided data from Statens Vegvesen (SVV) were given in several formats (*.dwg, *.dxf, *.xyz). However, both many modifications and a specific format of grid files were required in order to run the software DAN3D. For that purpose, many software had to be used. From the Autodesk platform, both AutoCAD and Civil 3D were mainly useful for the modification of the topography and the creation of grid files. DAN3D requires two DEM (Digital Elevation Model). The first file is called “*Topography File*” and it represents the topography of the examined area excluding the sliding mass. That DEM file contains points with different elevations of the original surface. However, there are two important areas that require special treatment (Figure 17). The first location is where the initial sliding mass starts. The elevation should be on the sliding surface and not on the original height, where it was before the landslide happens. As a result, a careful approach had to be done since there was no data available how did the area look like before the landslide event a few thousand years ago. The second location is at the area of the final deposition where the sliding mass had to be removed and the new elevations should be defined.

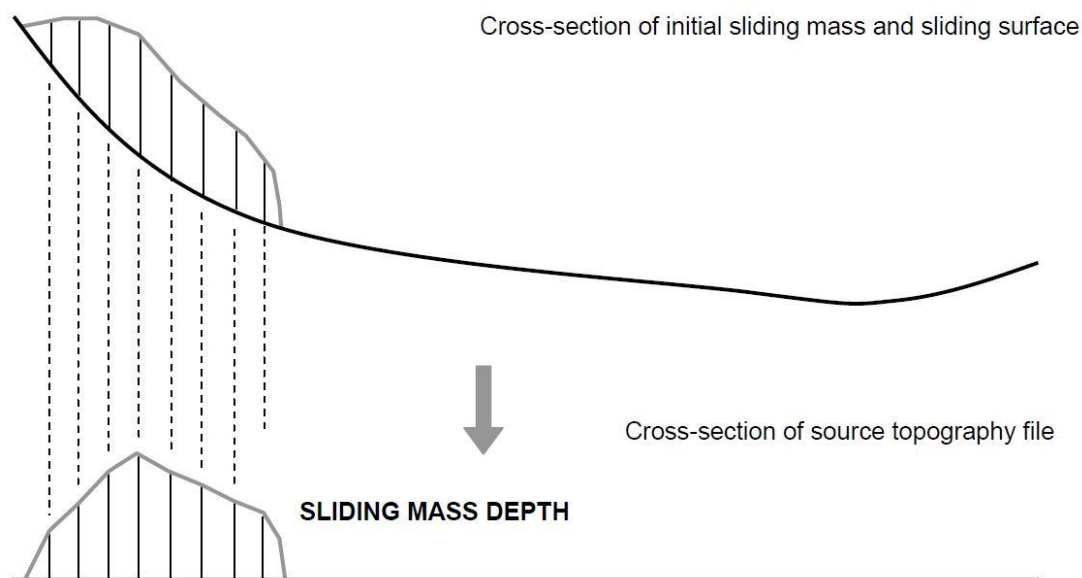


Figure 13: A typical cross-section of how does the “Source Depth” topography file look like

Contrarily, the “*Source Depth*” topography file, which is the second required file, contains the heights at the initial area and not the elevation of the sliding mass (Figure 13). The regeneration of that area was a very challenging task and a series of significant tasks should be completed. The first task was

the calculation of the volume of the sliding mass. For that purpose, some logical simplifications together with some simple geometry calculations were made (Figure 14). Based on the thickness of the slide new contours were created. The area included between the old and the new contour multiplied with the height difference of contours lines can give a rough estimation of the landslide's volume.



Figure 14: The white lines are the original contours, the green the new contours and the area (marked with yellow lines) multiplied with the contour difference can give a volume approximation.

The second and most challenging task was to restore the original topography by placing the sliding mass back in the initial position. The volume should be distributed proportional, so the regeneration of the initial topography to be as realistically as possible. Consequently, new contours were designed showing the new elevations after the replacing of the sliding mass at the original position (Figure 15).

Since the regeneration had been done, the third step was the determination of height in every point of the sliding mass. Height contours were created, based on the intersection of the old and the new elevation contours because at those points the height difference is known. The software AutoCAD from Autodesk platform was used for the completion of those tasks.

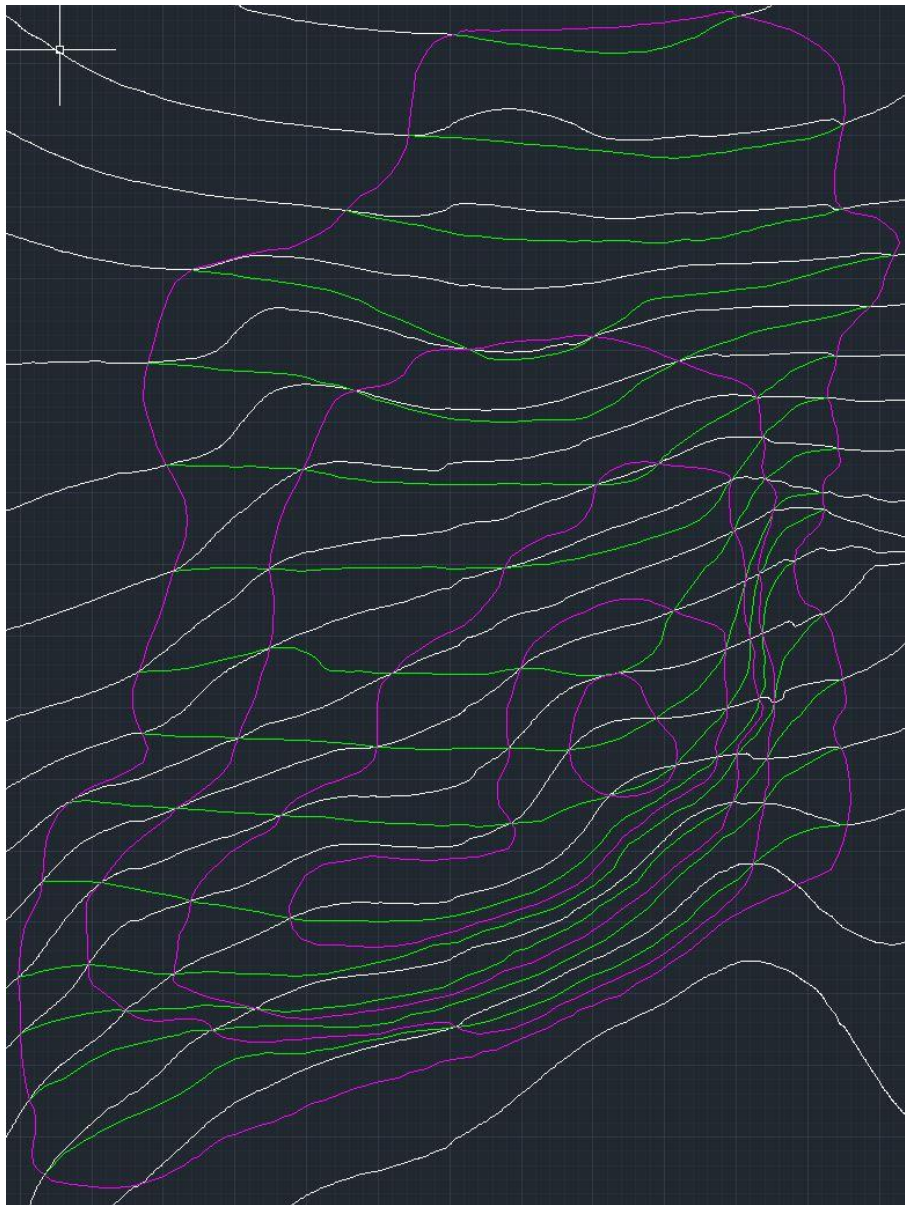


Figure 15: The white lines are the original contours, the green the new contours and the purple represent the height contours passing where the original and the new contours are intersecting because the height on those points is known.

For the final step of the procedure, another software from the Autodesk platform was used. The created files were modified with Civil 3D. Through that software two main goals achieved. The first was the creation of a surface, based on the contours, and the second was a grid, based on the surface. In the end, the points were exported in *.xyz files. The further processing of those files was done with the software Surfer11 from Golden Software Inc. Through Surfer11 those files were transformed into proper ASCII (American Standard Code for Information Interchange) grid files (see Appendix for details). Finally, the grid files were ready to be imported on DAN3D and the remaining part of the

process was the determination of the analysis' parameters. The final step was the evaluation and the editing of the result and it was done with Surfer11 (Figure 16).

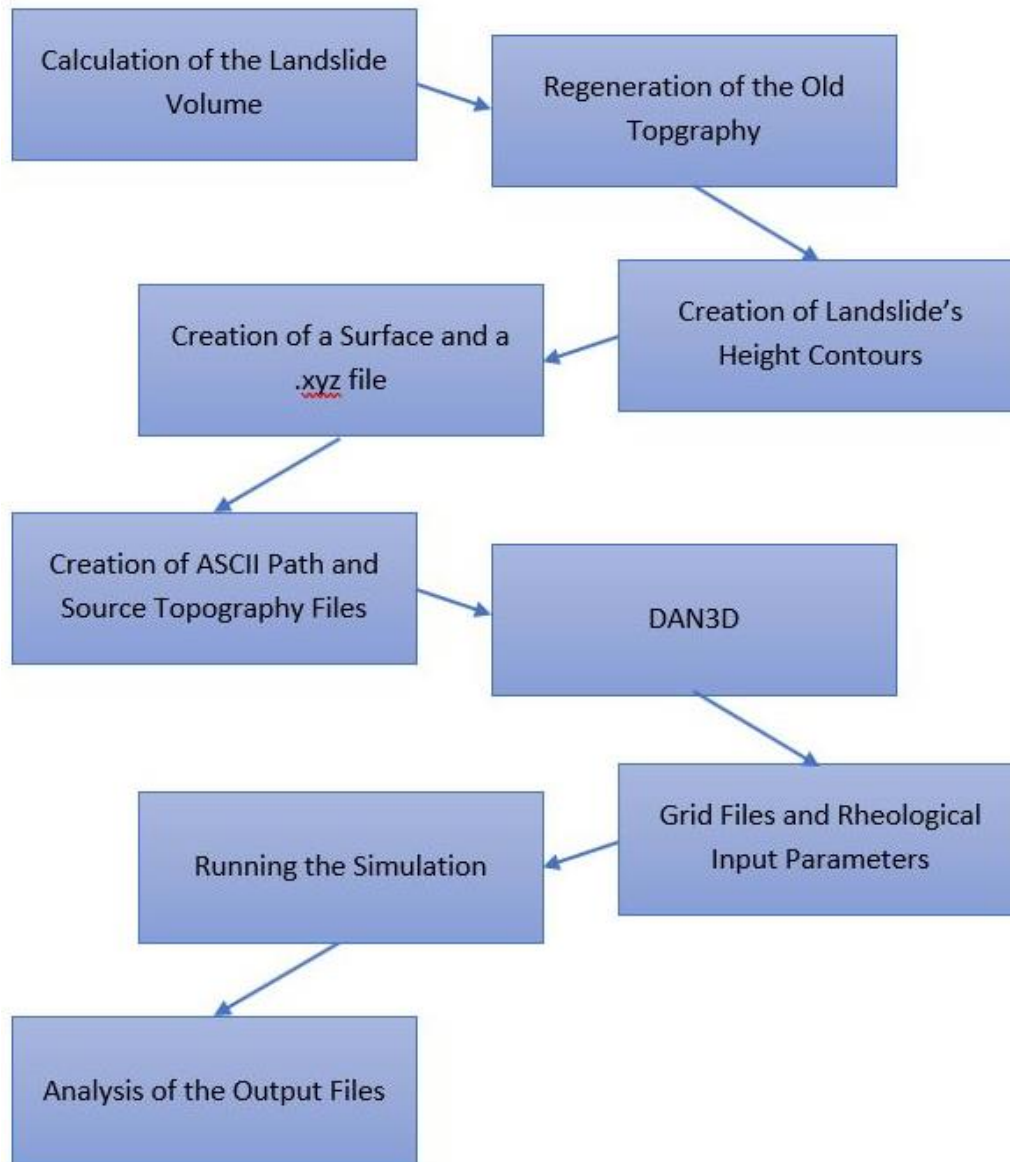


Figure 16: Procedure and flow chart for the DAN3D model simulations.

5.4. The Methodology of Analysis

Before the analytical calculation of the run-out distance was performed a careful estimation of the topography had to be made. Topography plays an essential role in the analysis result; consequently, the estimation should be as real as possible. It was a challenging and time-consuming process because

of the uncertainties of the examined case, which analytically are explained below. DAN3D requires two separate files for simulation. The first file is called “*Path Topography*” and it is an ASCII formatted digital terrain model, DTMs (*.GRD), grid file containing the elevations of the original terrain. However, some modifications in the elevations are required before the creation of that grid file. The sliding mass must be removed both from the release area and from the final deposition (Figure 17). Given the fact that the examined landslide happened some thousand years ago, the topography at the release area was ready but the identification of the sliding mass at the deposition was a tricky task. Aiming such modification requires a careful estimation of the sliding mass. Because of the uncertainties two alternative solutions were promoted and tested.

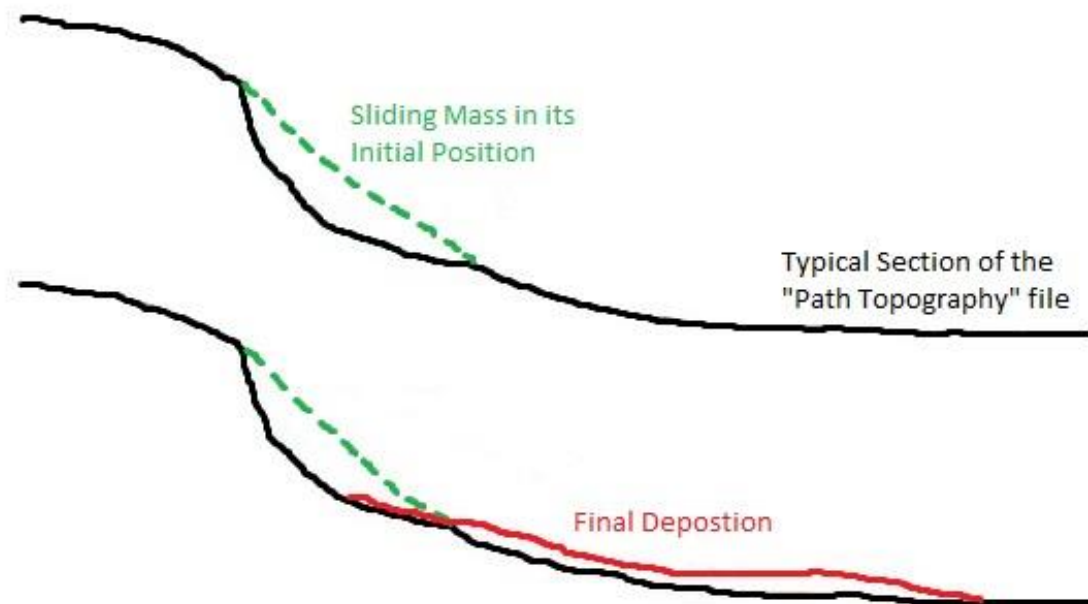


Figure 17: Black line shows a typical section of how the topography at the “*Path Topography*” file should look like and the green and red line represent the sliding mass at the release and final deposition area respectively.

The second file is called “*Source Depth*” and it is composed of the heights of the sliding mass (Figure 13). The creation of that file required a series of different steps. The first step was the identification of the release area and the regeneration of the original terrain before the event of the landslide with respect to the calculated volume. After “placing” the sliding mass back to its initial position (by creating new contours) the determination of the heights could become from the points where the old and the new contours are intersected (Figure 15). On those points, the elevation difference is the height of the sliding mass. As a result, a file with elevations of the sliding mass was ready. Because DAN3D requires an ASCII formatted digital terrain model, DTMs (*.GRD), grid file, software Surfer11, provided from Golden Software Inc., was used for the transformation to the desired format.

Last but not least, it was deemed that the bulking factor will be neglected because the effect on the final result will not be minor especially compared with all the other uncertainties of this problem.

After the creation of the grid files, the analysis parameters had to be defined. Both frictional and plastic rheological models require unit weight, maximum erosion depth and a parameter called “*Internal Friction Angle*” (Figure 18). Since in the present study is conducted in a preface stage, and for the effect of the erosion required an extensive study, it was considered that any effect of erosion will be neglected. Consequently, that parameter is set equal to zero.

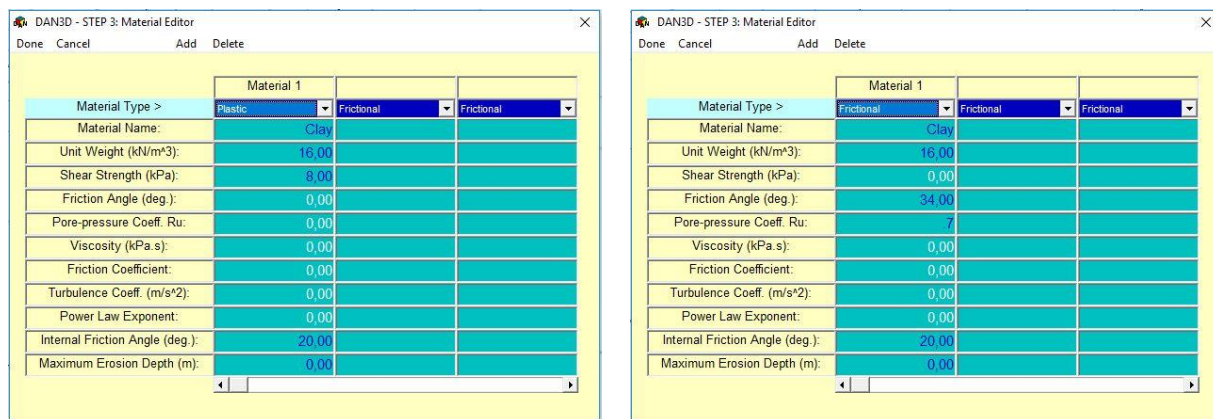


Figure 18: DAN3D Input Parameters using Plastic Rheological Model (left) and Frictional Rheological Model (right).

DAN3D considers that the internal rheology of the material is assumed to be frictional. The governing parameter is called “*Internal Friction Angle*” and it is an angle that defines how much of internal friction there is in a material (Hungry 2010). The tangential stress coefficients k_x and k_y included in an expression presented by Savage and Hutter (1989) are derived by using the internal friction angle. The software considers that while the materials are deforming internally are behaved as frictional. The explanation of that in a microscopic scale is that for every individual particle, the shear deformation is increasing and decreasing with the same rate with the normal stress which is posed to itself. Software suggestion, for dry fragmented rock, is 35 degrees which is the default value as well and 0 degrees for fluids. Finally, Hungry (2010) suggests that the user can experience using different values for the simulation.

According to NGI (2017) and NGI (2016), the unit weight (γ) is 16 kN/m³. However, the parameter “*Internal Friction Angle*” was unknown and its effect on the analysis was not determined. Consequently, a sensitivity analysis was conducted in order to determine it. The results showed that there was no big deviation on the run-out distance and a mean value of 20 degrees was decided to be used in all analyses, which was also a value suggested from similar studies (Gebreslassie 2015). At Figure 19, 4 groups of lines are shaped. Each group has 5 lines. The lines within the groups have the

same shear strength but different internal friction angles. As a result, no matter what the value of the internal friction angle is, the final run-out distance is similar. Consequently, it is obvious that the internal friction angle does not play a significant role in the determination of the run-out distance. Consequently, the assumption the internal friction angle is equal to 20 degrees seems even more reasonable.

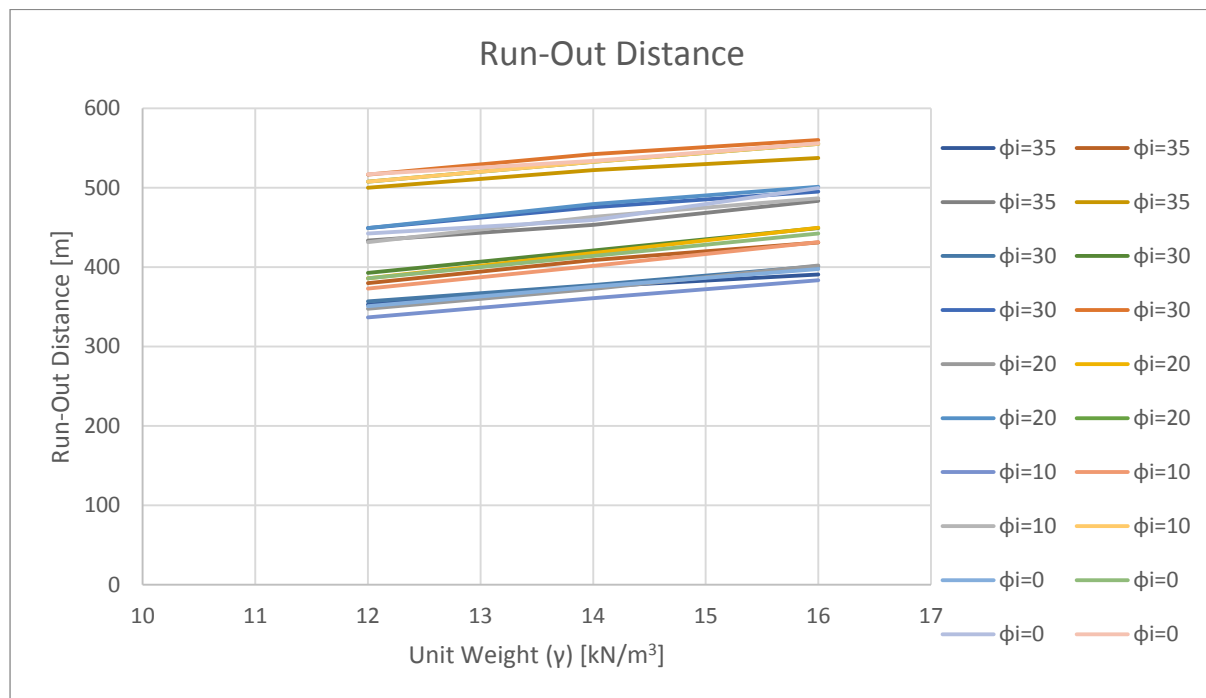


Figure 19: Every group of lines can be considered as an individual line because no matter what the internal friction angle is, the run-out distance is not affected so much. Parameters like shear strength and unit weight play a more significant role at the determination of the final result.

As far as the plastic rheological model is concerned, the only missing parameter is “*Shear Strength*”. A remoulded shear strength value was used since the material will be remoulded during an event of a debris flow. There were different values proposed because the shear strength is increasing with depth (Figure 20). The maximum depth of the sliding mass is not exceeding the depth of 20 meters. As a result, remoulded shear strength could have a maximum value of 10 kPa. Not being sure what would a proper value be, several values from 1 up to 10 kPa were used on the simulations.

Continuing to frictional rheology material four parameters, “Unit Weight”, “Friction Angle”, “*Pore-Pressure Coefficient*” and “*Internal Friction Angle*”, had to be defined. The internal friction angle was kept the same as the previous model. The unit weight is decided to be equal to 16 kN/m³ based on the previous set of analyses. As far the friction angle is concerned, a value of 32 degrees was suggested from (NGI 2017). However, other values close to it were used as well.

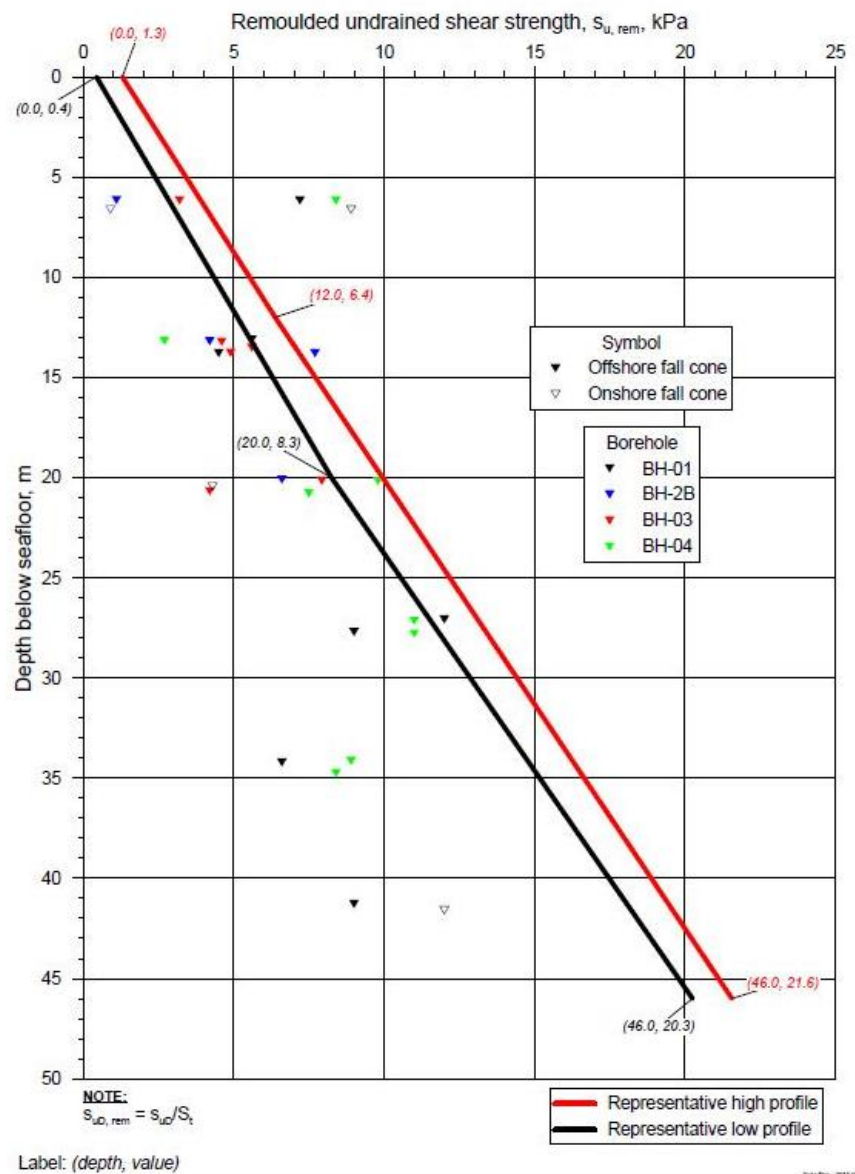


Figure 20: Linear increase of the remoulded shear strength with depth.

Finally, the determination of the pore-pressure coefficient (R_u) was a challenging task. The pore-pressure coefficient is defined as the ratio of pore pressure with total stress. An estimation with some rough hand-calculations was made. In a hypothetical case where the pore pressure follows a hydrostatic distribution with a unit weight of 20kN/m^3 , the pore-pressure coefficient (R_u) is equal to 0.5 and that set as the lower limit of R_u . At the present study, the unit weight is less, therefore R_u is higher. In case that the pore-pressure gradient is higher than the hydrostatic R_u is again more than 0.5. Additionally, no suction is observed at the seabed, as a result, a starting value of 0.5 was selected and some higher values (until 0.8) were used as well. The pore-pressure coefficient was calculated this

way because in DAN3D the drag force from the water was not possible to be inputted. Consequently, the pore-pressure coefficient had to be as realistically as possible because the simulated landslide is submarine but the simulation was conducted as a normal debris flow landslide.

Concerning the sequence of the analysis steps, the first goal was to clarify which of the two proposed topographies matched and could simulate better the real case. The plastic rheological model used for that process because it was the simplest rheological model and the provided parameters from the geotechnical report (NGI 2016) had a perfect match with the required inputted parameters. After selecting topography, the plastic rheological model was tested. In parallel, a comparison was conducted with NGI (2017) by using the same parameters wherever it was possible. NGI used a different rheological model; consequently, the comparison of two different models using similar parameters was a significant task to be done.

Last but not least, there was the last set of analysis parameters to be defined and that was the computational parameters. Those parameters were set according to the literature report and DAN3D's manual (Hungr 2010). The first step was to open the "Control Parameters" dialog box (Figure 21) and input some name defining information about the software together with other computational parameters like erosion rate, maximum simulation time and the time step is set as well on the same dialog box. Furthermore, the maximum simulation time and time step in seconds could be selected. The default values were 1000 and 0.1 seconds respectively. However, the maximum simulation time could be adjusted in the beginning or/and anytime during the simulation or/and just before the simulation ends. Concerning the time step, a typical range could be between 0.05 and 0.1 seconds but its determination could be only done before the simulation starts. Higher values could be set as well, decreasing, of course, the precision of the results (Hungr 2010). Since there was no other tool, apart from the completion of the maximum simulation time, to stop an analysis, either the user had to estimate the required amount of time or the default values had to be kept. According to previous experience and based on the advice of experts on the software, the maximum simulation time was adjusted for every different case and if more it was required, it was added during the simulation. That saved a lot of precious computational time and gave the opportunity of conducting several simulations in the given period.

Proceeding to the next dialog box, the two ASCII formatted digital terrain models, DTMs (*.GRD), grid files had to be inputted to the software. The process of creating those two files is analytically described above. Both files had to have the same grid size and spacing. Even if the advice from the developers was to relocate the starting point of x- and y- coordinates to (0,0) to minimize the risk of a precision mistake due to the large numbers which are usually met on geographical coordinates (Hungr 1995), the original coordinates were kept for having a direct match with the provided results from NGI (2017). Additionally, it was possible to add an erosion file on this dialog box, but erosion

concept was neglected on the present study. The last set of the opening dialog boxes sequence named “Material Editor” (Figure 21) and that is where the geotechnical parameters had to be inputted and it had already discussed.



Figure 21: “Control Parameter” (left) and “Grid File Assignment” (right) dialog boxes.

There is a couple of dialog boxes that has to be discussed and they concern the selection of the output files and some last computational parameters. The dialog box, named “Data Output Options” (Figure 22), provides the option of selecting the desired output files and the location where the output files will be saved. Given the fact that the present study examines only the run-out distances, the selected output files were “Nodal depths (depth.grd)” and “Nodal elevations (surf.grd)”.

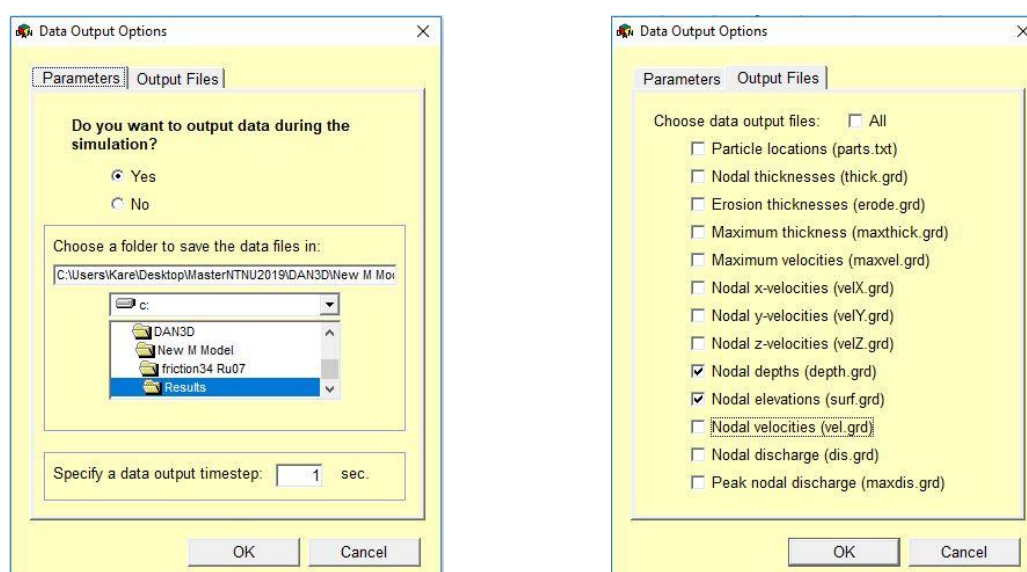


Figure 22: “Data Output Options” dialog box. The “Parameters” tab (left) shows the location of the saved output files and the “Output Files” tab (right) shows the selected output files.

The last dialog box which had to be set is called “*Options*” (Figure 23). There was an inconsistency between the software’s manual (Hungry 2010) and reality. The default value of “*Velocity Smoothing Coefficient*” according to the manual had to be 0.01 but it was 0.00. The same problem existed in a previous study (Yifru 2014) and the results showed that the final outputs were closed enough regardless of the value of “*Velocity Smoothing Coefficient*”. In order to be in accordance with the manual’s guidelines the selected value of “*Velocity Smoothing Coefficient*” set equal to 0.01. All the other parameters were kept as default values.

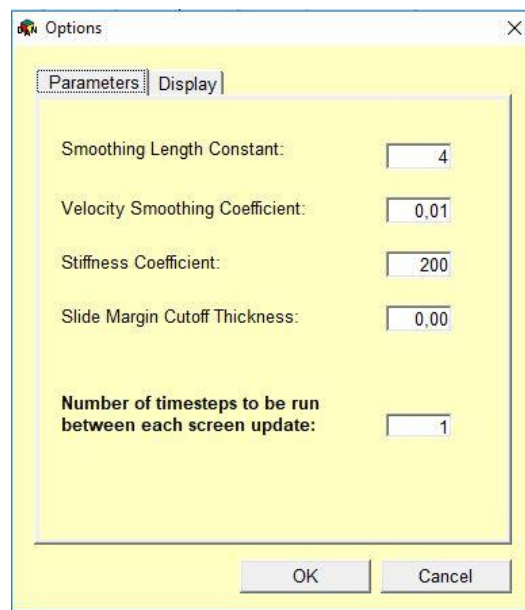


Figure 23: “*Options*” dialog box showing the values which have been used for the simulations.

5.5. Results

The back-calculation of the landslide was conducted with the utilization of two simple rheological models. Both the plastic and the frictional rheological models, which were the chosen models, gave realistic results. The selection was based on the simplicity of the models. Since there were not available laboratory data concerning the rheological parameters of the soil, it was deemed that simpler rheological models would give a more realistic representation of the landslide and should also be compared with the results from NGI’s study.

5.5.1. Plastic Rheological Model

For the first set of analyses, the plastic rheological model was chosen. The reason for this was to test which of the two promoted topographies could better represent the landslide (Figure 24). Additionally, the plastic rheological model was the simplest rheological model and the required parameters were matching perfectly with the given ones from (NGI 2017). Table 1 shows the selected values for the back-calculation analysis. After every simulation extensive editing took place. The run-out distance was measured from the crown of the landslide until the farthest edge of the landslide deposition (Figure 8).

Unit Weight (γ) [kN/m³]	12, 14, 16
Remoulded Shear Strength (Su_{rem}) [kPa]	1, 2, 3, 4, 5, 6, 7, 8, 9 , 10
Internal Friction Angle (ϕ_i) [degrees]	20

Table 1: The values of the parameters which have been used for the back-calculation of the landslide. With bold the values which gave the best fit.

The simulation results, from the 1st topography alternative, were satisfying but there was some deviation from the actual shape (Figure 28). The final run-out distance was 512.2 meters. That result was achieved using a remoulded shear strength of 9 kPa. The progression of that landslide follows a path similar to the actual landslide. However, it turns to the right and the bottom part of the landslide seems to be more spread than the original. Additionally, an important detail must be mentioned. In Figure 24, there is no solid data concerning the thickness of the landslide. However, from profiling data, provided by NGI (2017), the thickness varies from 0 to 2 meters at the first 100 meters of the deposition and around 2 meters for the rest of the deposition. The snapshots taken from Surfer11 had to be edited in a specific way in order to be presentable. Consequently, a minimum thickness of 0.5 meters had to be chosen. As a result, there is an area that appears to have no material from the sliding mass. However, the thickness of the sliding mass in that area is less than half a meter.

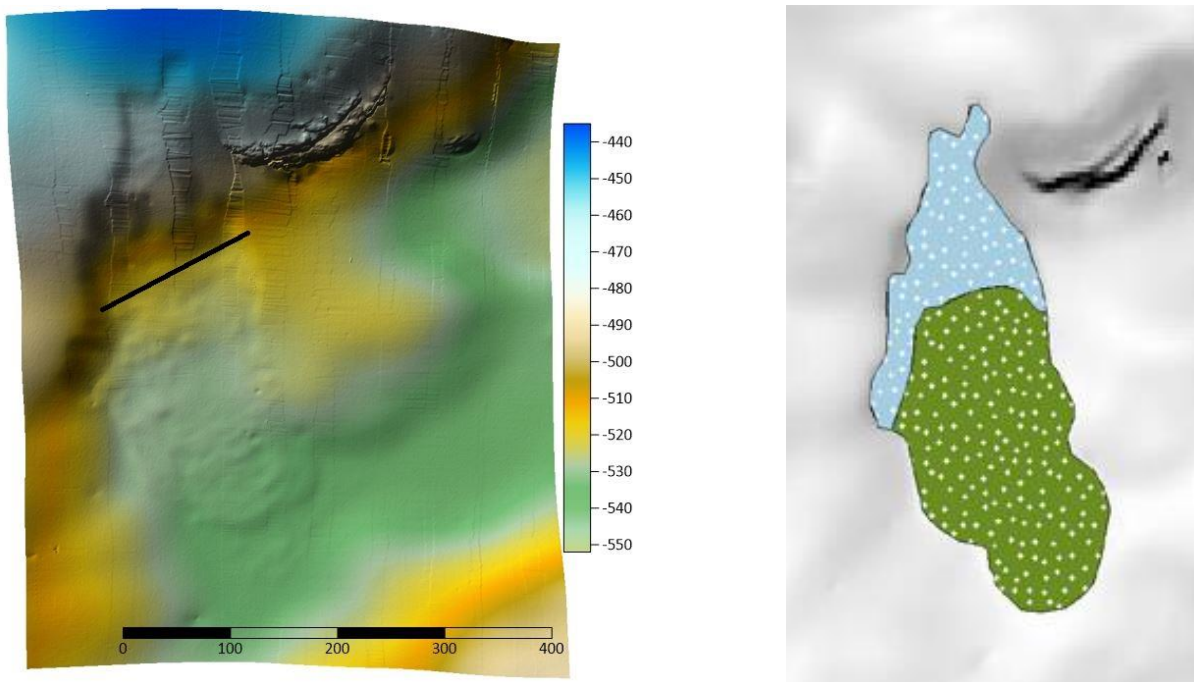


Figure 24: (Left) Geomorphology of submarine landslide (Bjørnafjorden, Norway). The black line separates the release area with the final deposition area. (Right) The original shape of the landslide as it is shown in NGI (2017).

The 2nd topography alternative gave more realistic results (Figure 29). The result, in this alternative, was achieved with a remoulded shear strength of 8 kPa. Even if the width of the final deposition is larger than the original, the path and the run-out distance are similar, around 502 meters, to the original landslide (Figure 25). Both topographies meet around 8.5 kPa in terms of run-out distance. However, the second alternative could combine a more realistic representation of the landslide in terms of shape and a combination of a more accurate set of geotechnical values. Consequently, the 2nd topography was used for further simulations because it could simulate the progression of the landslide better.

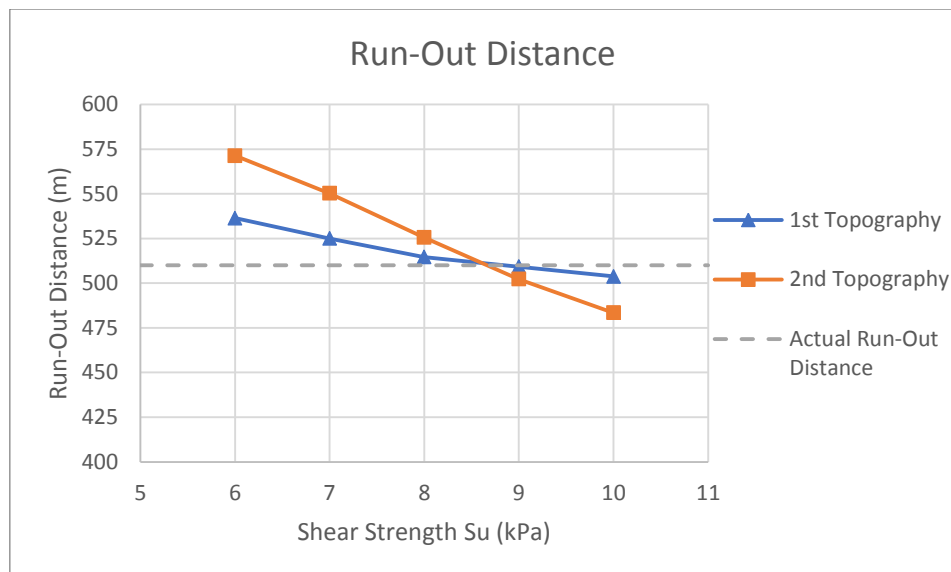


Figure 25: Comparison of the run-out distances of the two alternative topographies.

The best combination (Table 1) was given with remoulded shear strength of 9 and 8 kPa for the first and second alternatives respectively. As a result, a comparison on the maximum flow velocity and the average thickness was made in order to evaluate how the landslide is progressing during the motion. Both magnitudes are close, showing that the evolution of both events is similar (Figure 26).

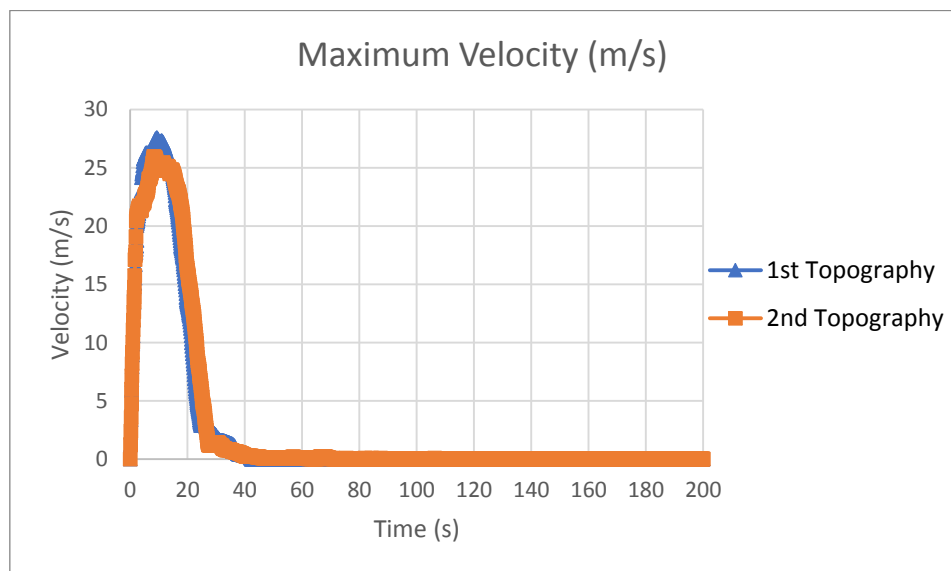


Figure 26: Comparison of the maximum velocity and how it evolves with time in both alternative topographies.

The average thickness is around 7 meters in the beginning and around 1.2 meters after the completion of the event (Figure 27). According to some rough estimation, the affected area from the sliding mass

was calculated around 100000 m^2 . Given the fact the total volume of the sliding mass is around 170000 m^3 , the affected area from both simulations is calculated around 140000 m^2 . This shows that the mass has spread more than the actual landslide. The fact that the final deposition was spread more than the actual is also illustrated in Figure 28 and Figure 29.

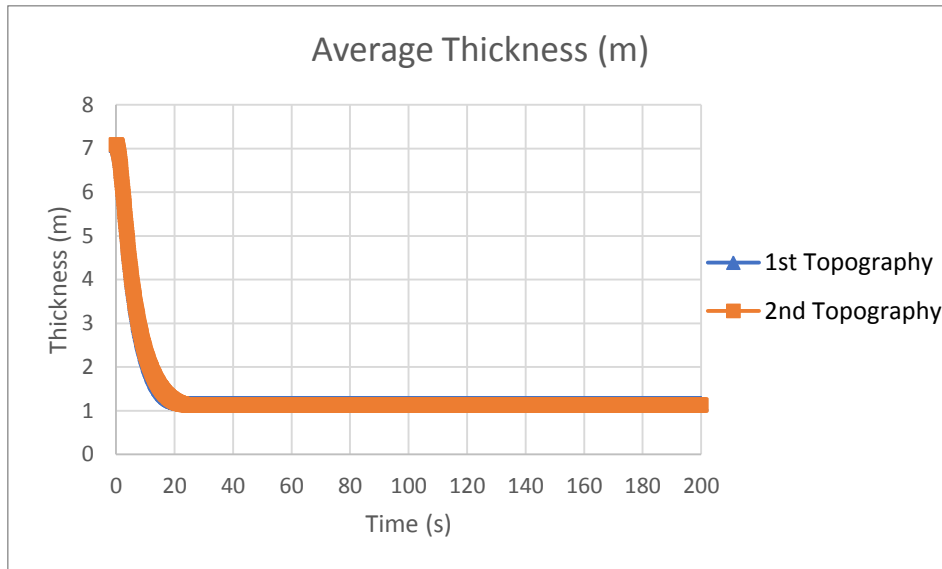


Figure 27: Comparison of the average thickness and how it evolves with time in both alternative topographies.

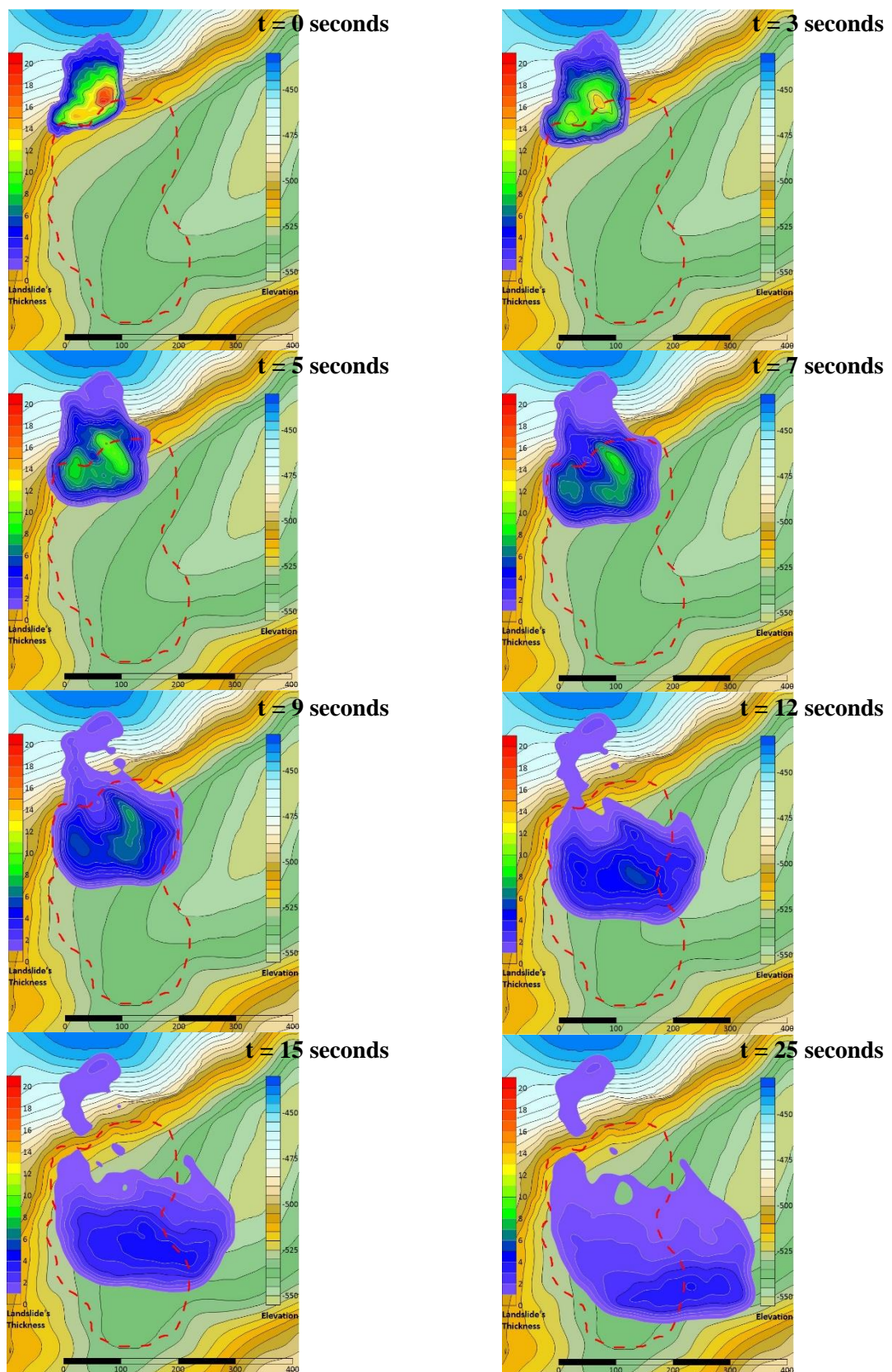


Figure 28: Landslide progression on the 1st Topography alternative. Flow thickness contours at 0, 3, 5, 7, 9, 12, 15 and 25 simulation time (seconds) using plastic rheology. Legends show the thickness of the landslide (left) and the elevation (right). The red dashed line shows the limits of the actual deposition of the landslide.

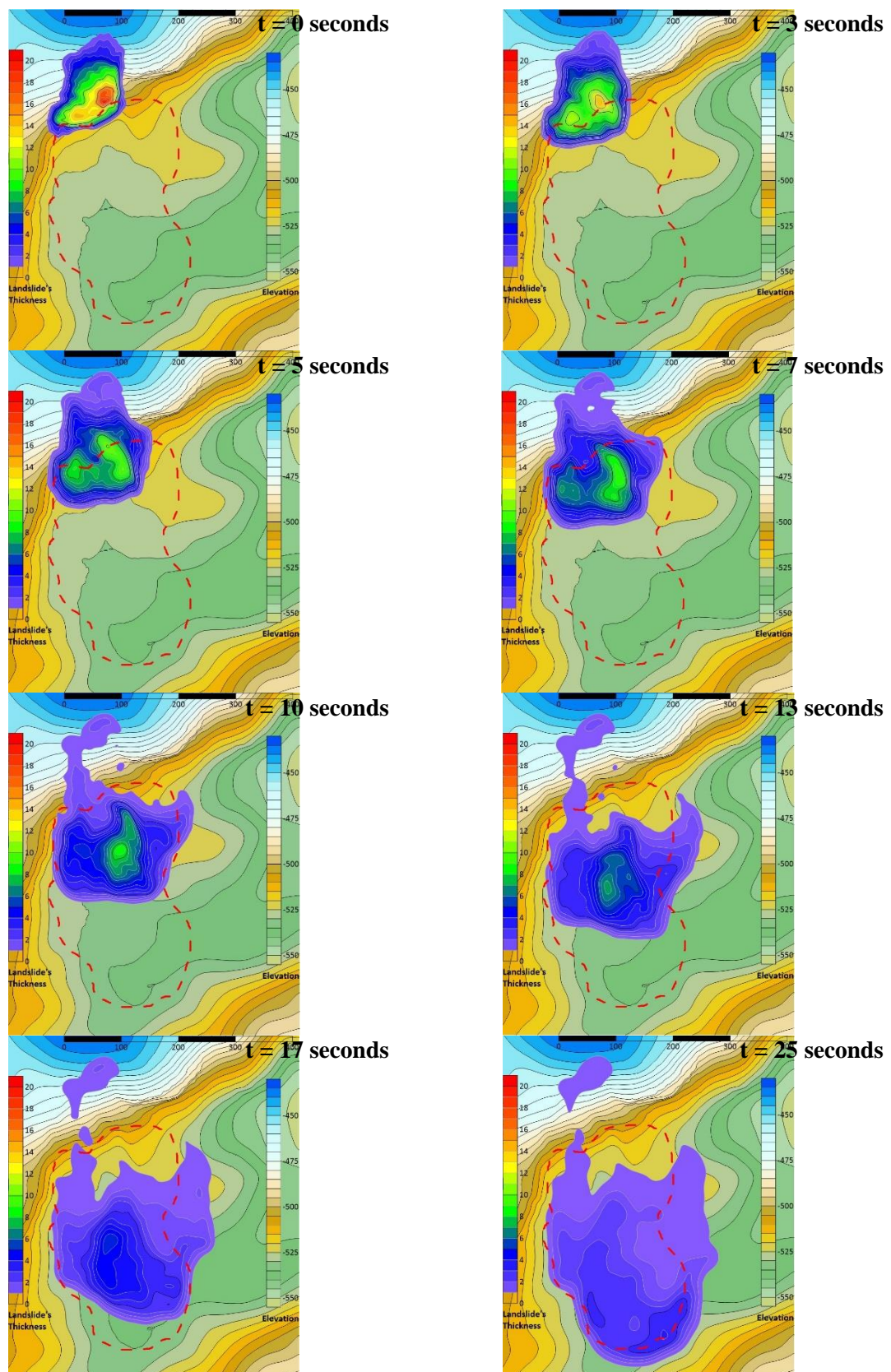


Figure 29: Landslide progression on the 2nd Topography alternative. Flow thickness contours at 0, 3, 5, 7, 10, 13, 17 and 25 simulation time (seconds) using plastic rheology. Legends show the thickness of the landslide (left) and the elevation (right). The red dashed line shows the limits of the actual deposition of the landslide.

5.5.2. Frictional Rheological Model

The frictional rheological model was compared with the plastic rheology mode. Additionally, the frictional rheological model was checked on how realistically it can simulate the progression of the landslide. The required parameters in the frictional rheological model were the friction angle (φ) and the pore-pressure coefficient (Ru). Table 2 shows the selected values for the back-calculation analysis. The unit weight was kept equal to 16 kN/m^3 , due to the fact that it gave the best matching from the previous results.

Unit Weight (γ) [kN/m^3]	16
Friction Angle (φ) [degrees]	30, 32, 34
Pore-Pressure Coefficient (Ru) [-]	0.5, 0.6, 0.65, 0.7, 0.75 , 0.8
Internal Friction Angle (φ_i) [degrees]	20

Table 2: The values of the parameters which have been used for the back-calculation of the landslide. With bold the values which gave the best fit.

For every conducted simulation, the run-out distance was measured (Figure 30). The best simulation of the landslide was achieved with the combination shown in bold text in Table 2. The simulated run-out distance (around 510 meters) was perfectly matching with the actual distance. Furthermore, the shape of the deposition was realistic and representative (Figure 33).

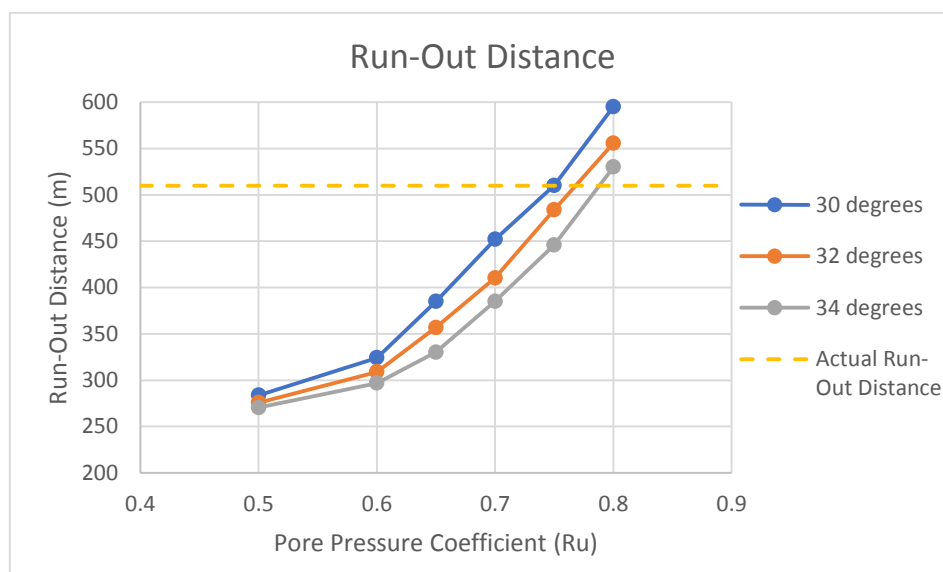


Figure 30: Comparison of the run-out distances with the frictional rheological model.

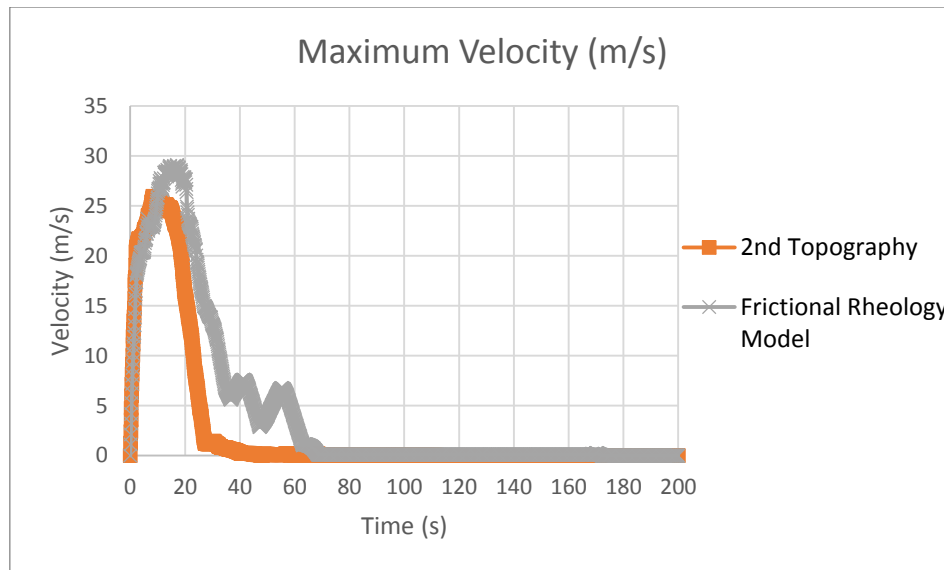


Figure 31: Comparison of the maximum velocity between the plastic and the frictional rheological model.

Contrary to the plastic rheological model, the maximum velocity is higher, and the duration of the event is around 25 seconds bigger (Figure 31). The variation of the velocity is peculiar, and it is related to the topography. As far as thickness is concerned, the final deposition is thicker (around 1,8 meters) (Figure 32). Following the same calculation procedure as previously, the affected area is close to the actual landslide 95000 m^2 .

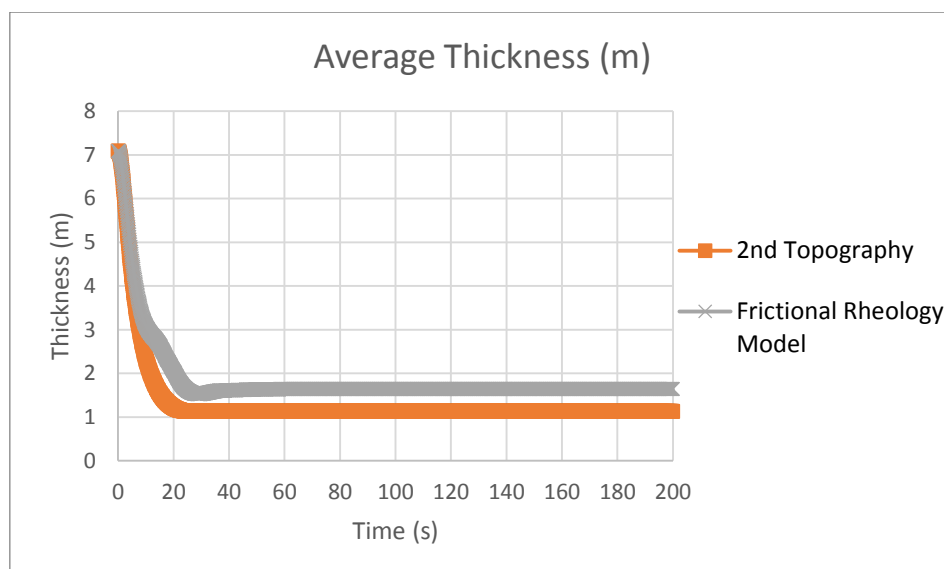


Figure 32: Comparison of the average thickness between the plastic and the frictional rheological model.

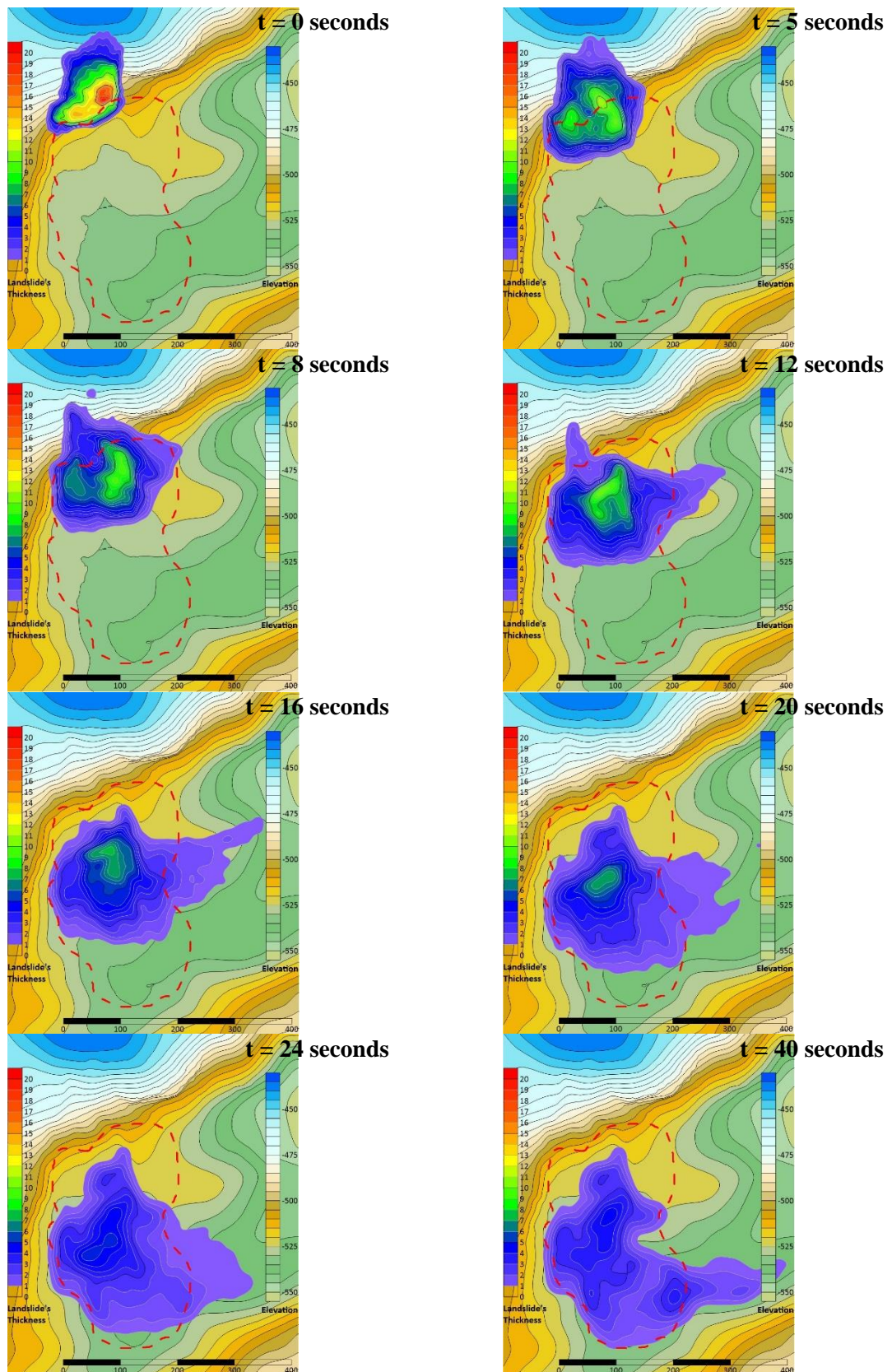


Figure 33: Landslide progression with the frictional rheological model. Flow thickness contours at 0, 5, 8, 12, 16, 20, 24 and 40 simulation time (seconds) using plastic rheology. Legends show the landslide's thickness (left) and the elevation (right). The red dashed line shows the limits of the actual deposition of the landslide.

5.6. Comparison with NGI's Results

5.6.1. Description of BING's Model

Given the fact that NGI has already studied this landslide, a comparison would be very interesting. This comparison would be useful since different models and software were used to study the same landslide. It was interesting to check how different approaches could meet and how different models and parameters could simulate a given landslide. The model which was used by NGI (2017) is suitable for cohesive soils. Hershel-Bulkley rheology expression governs the movement of the sliding mass. That rheological model controls the non-linear relationship between the strain and the stress (Equation 37). A Lagrangian scheme has been used to solve the equations, which allows the grid to be deformed during the flow.

$$\left| \frac{\dot{\gamma}}{\dot{\gamma}_r} \right|^n = \begin{cases} 0, & |\tau| \leq \tau_y \\ \frac{\tau}{\tau_{y,s} gn(\dot{\gamma})} - 1, & |\tau| > \tau_y \end{cases} \quad (37)$$

where $\dot{\gamma}$ is the strain rate, $\dot{\gamma}_r$ is a reference strain rate based on Equation 38, τ is the shear stress and τ_y is the shear yield stress

$$\dot{\gamma}_r = (\tau_y / \mu)^{1/n} \quad (38)$$

where μ is the dynamic viscosity. Equations (37) and (38) control the ratio depth versus height of the shear and plug layers in the fluid.

The used software (BING3) is a property of NGI and it is suitable for visco-plastic flows. There are several extensions of that software (Imran, Harff et al. 2001), (Blasio, Engvik et al. 2004) and (Blasio, Elverh b i et al. 2004). In the movement of the mass (Figure 34), there was a plug layer rides the shear layer, and its thickness was determined by the height of the flow and the material's yield stress. The model that NGI used was specifically developed for submarine conditions. Other parameters considered were hydrostatic pressure, the friction drag and the strength reduction during run-out.

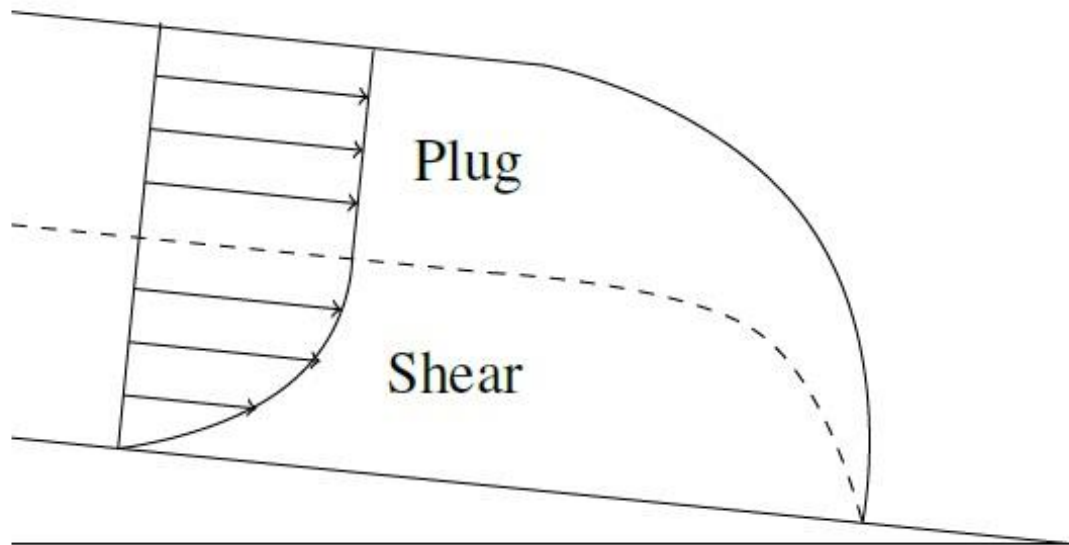


Figure 34: This drawing shows the components of a debris model. The Shear layer is at the bottom of the flow and the plug layer is above and plowing the slip plane.

5.6.2. Parameters of BING's Model

Phenomena like erosion and entrainment of the seafloor were ignored and the parameters taken into account were the initial yield strength $\tau_{y,s}$, the remoulded yield strength $\tau_{y,r}$, the remoulding coefficient Γ , the kinematic viscosity ν , the Herschel-Bulkley exponent n , pressure drag coefficient C_P and the friction drag coefficient C_{FR} . The values which gave the best fit with the landslide after the back-calculation are presented in Table 3.

Parameter	Value	Unit
$\tau_{y,s}$	8	kPa
$\tau_{y,r}$	1.5	kPa
Γ	0.1	–
ν	0.25	m ² /s
n	0.15	–
C_P	0.5	–
C_{FR}	0.005	–

Table 3: Best-fit parameters for the landslide back-analysis from NGI's back-calculation.

The basal shear stress (τ_y) is directly dependent on the initial yield strength ($\tau_{y,s}$) and the remoulded yield strength ($\tau_{y,r}$). The initial yield strength is the shear strength that the material has exactly before the landslide start. The remoulded yield strength is the fully-remoulded strength of the soil, which can be affected by soil water content. The remoulding coefficient (Γ) governs the reduction of the yield shear strength (τ_y) in relation to the initial and remoulded shear strength. The equation below expresses the reduction of the yield shear strength (Equation 39). A typical range of values is from 0.001 to 0.1.

$$\tau_y = \tau_{y,r} + (\tau_{y,s} - \tau_{y,r}) \exp[-\Gamma \cdot \gamma] \quad (39)$$

Kinematic viscosity is a parameter that shows the resistance of the movement to shearing. A typical value for submarine debris flows is 0.25 m²/s. The Herschel-Bulkley exponent (n) determines what kind of rheology the flow follows. If the Herschel-Bulkley exponent (n) is equal to 1 then the rheology is transformed to Bingham flow. For submarine landslides, a typical range is from 0.10 to 0.15. Finally, the pressure drag coefficient (C_P) and the friction drag coefficient (C_{FR}) govern the shape and the roughness at the top of the sliding mass, respectively.

5.6.3. Comparison of Models

In the present study, simple rheological models and various expressions and inputted parameters were used for the back-calculation of the landslide. However, it was deemed necessary to examine how the plastic rheological model behaves using the same parameters as NGI. As previously mentioned, there were two alternatives promoted but only the 2nd alternative was tested with the parameters that NGI used. In Table 3 the remoulded shear strength is equal to 1.5 kPa. This is the only common parameter with the plastic rheological model. As a result, unit weight (γ) and internal friction angle (ϕ_i) were kept the same as the previous analyses.

The results were peculiar (Figure 35) with both positive and negative aspects. The sliding mass seemed to oscillate among the two opposite slopes and in the end, it was stabilized in the area in between. Furthermore, the final deposition was spread in a wide area and the run-out distance was difficult to be measured.

However, the final location of the deposition was close to the original landslide. The shape of the deposition and the covered area gave a realistic representation of the seabed. Additionally, the run-out distance was estimated at around 502 meters, which was close to the examined landslide.

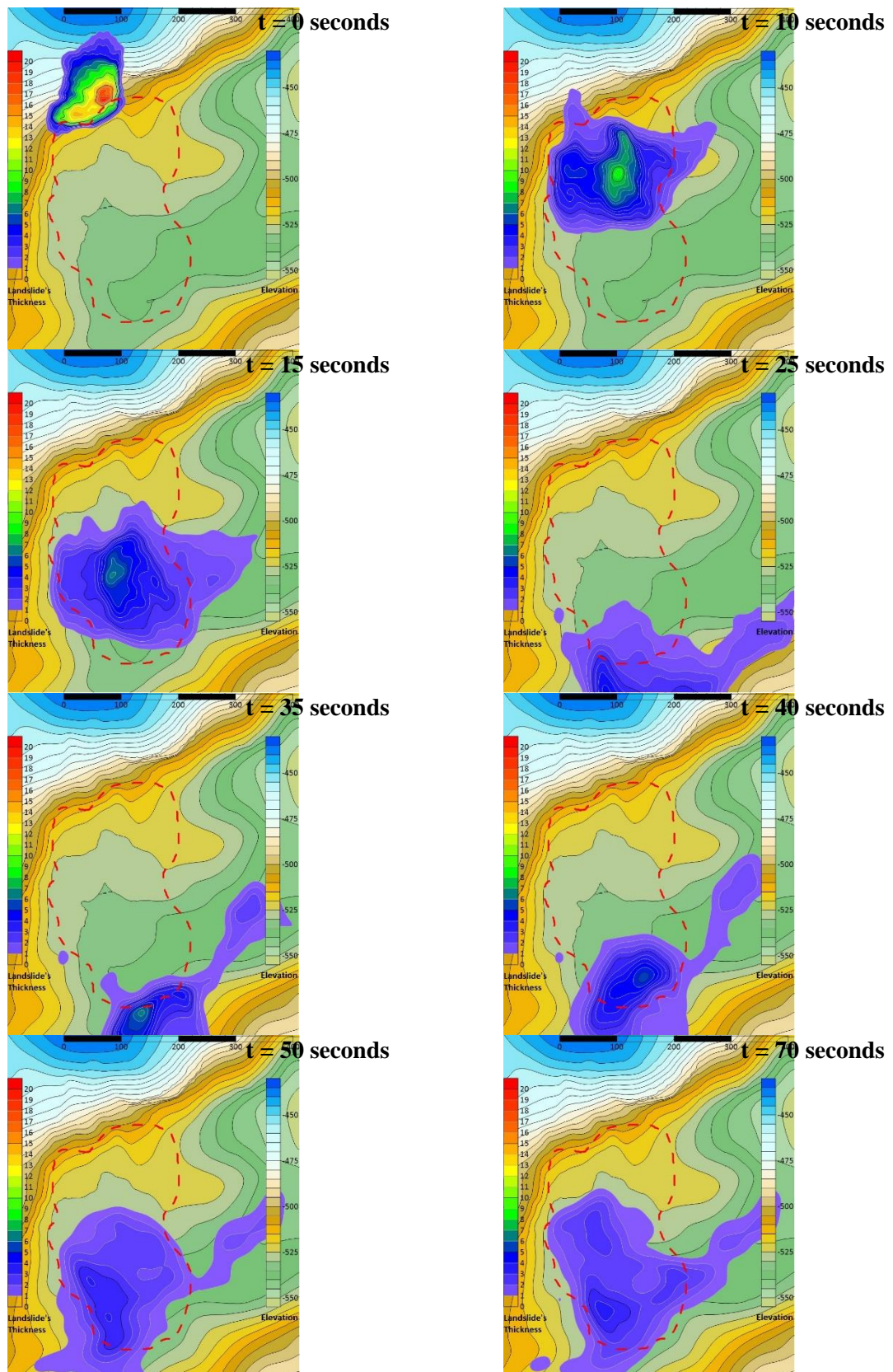


Figure 35: Landslide progression on the 2nd Topography alternative. Flow thickness contours at 0, 10, 15, 25, 35, 40, 50 and 70 simulation time (seconds) using plastic rheology. Legends show the landslide's thickness (left) and the elevation (right). The red dashed line shows the limits of the actual deposition of the landslide.

As mentioned above, the sliding mass seemed to oscillate between the two opposite slopes. This is also visible at maximum speed (Figure 36). The two velocity peaks show the oscillation. Moreover, the sliding mass' velocity zeros after 100 seconds (simulation time). This shows that the event lasts longer due to that oscillation.

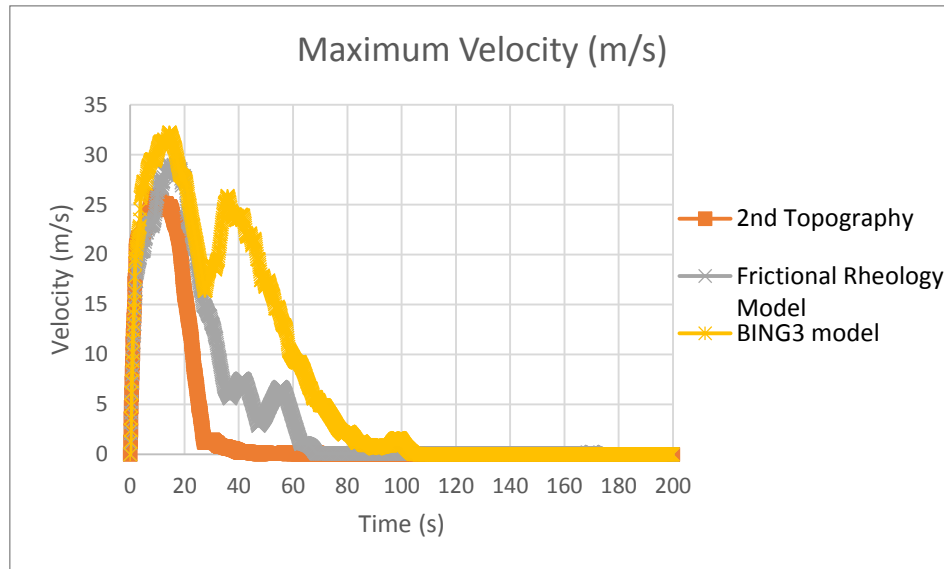


Figure 36: Comparison of the maximum velocity between the plastic, the frictional rheology, and the BING3 model.

Concerning the average thickness (Figure 37), the analysis with the parameters used in the BING3 model, gave a very thin layer of deposition of an average of 0.65 meters. Given this, showing that the spread of the sliding mass was very large, especially compared with the previous sets of analyses indicates, that the final shape of the main body of the sliding mass was close to the original one.

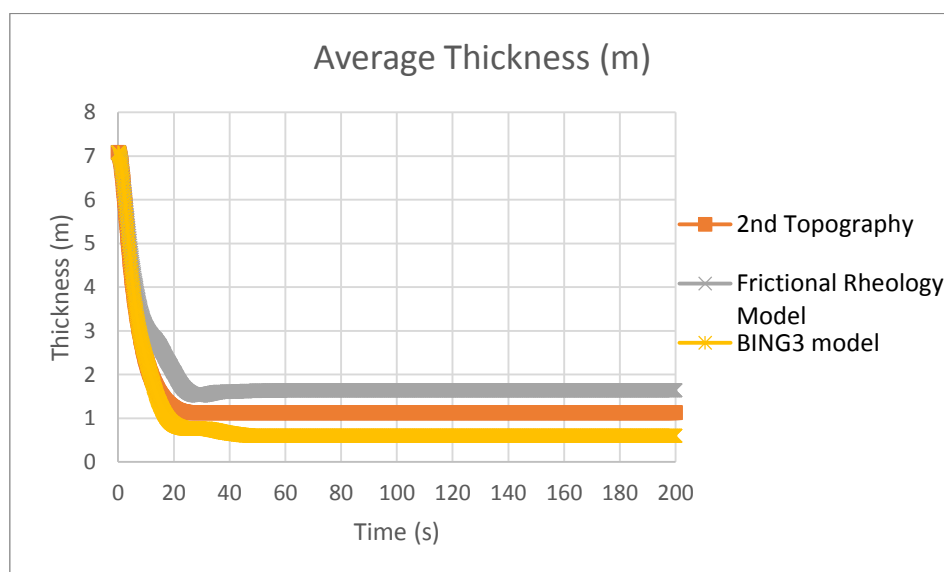


Figure 37: Comparison of the average thickness between the plastic, the frictional rheology, and the BING3 model.

6. Discussion of Results

6.1. Introduction

All of the observations from the study results are presented in the present chapter. Many simulations were made, and the results were both useful and peculiar. Different rheological models were used, and a comparison with NGI results was conducted as well. All of the observations from DAN3D with detailed explanations for each simulation case are also included in the present chapter.

6.2. Empirical Approach

The first step of the analysis was the approach of the run-out distance with different empirical expressions. Several approaches were examined due to the lack of expressions concerning submarine landslides. The estimation of the run-out distance was based on simple and easily measured (compared to other) parameters such as the height of slope or volume of the sliding mass. The first approach was made with a general expression made for different types of landslides. The run-out

distance was underestimated and as a result, more targeted approaches were necessary. Consequently, expressions developed for debris flows or expressions for landslides triggered by earthquakes were found, and the run-out distance's approach was better. Finally, two approaches based on the volume of the landslide were made with similar results.

Previous approaches were underestimating, even slightly, the actual run-out distance. However, Rickenmann (1999) developed an equation based on the combination of the slope's height and landslide's volume. This final approach slightly overestimated the run-out distance, but it was close to the actual one.

6.3. Numerical Calculation of Run-Out Distance

After the establishment of an upper and a lower limit from the empirical approach, the next step was the analytic back-calculation of the landslide. DAN3D had used for the regeneration of the landslide. The first step was the adoption of one of the two promoted topographies. The plastic rheological model was used. The reason for choosing this rheological model was the simplicity concerning the requirements for inputted parameters.

Subsequently, the frictional rheological model was used, and a comparison between the two rheological models was made. The final step was a comparison with NGI's results. NGI used different software (BING3) and rheological models, but the comparison was deemed necessary in order to analyze the results from two different approaches on the same subject.

A fundamental step, before any back-calculation took place, was conducting a sensitivity analysis examining the effect of the internal friction angle on the final result. The internal friction angle (φ_i) is the governing parameter concerning the internal rheology of the fluid (see details in Chapter 4). The sensitivity analysis showed that the effect of the internal friction angle was not significant (Figure 19). A value of 20 degrees was selected based on literature and the suggestions from software developers (Hungri 2010).

6.3.1. Plastic Rheological Model

Based on NGI (2016) and NGI (2017), the maximum value of the remoulded shear strength of the seabed's soil material was around 10 kPa. The best results were given with 8 and 9 kPa for the two promoted alternative topographies. According to Figure 25, both lines intersect exactly on the value of

510 meters, which was the actual run-out distance. Furthermore, the corresponding value of the shear strength in the intersection point was 8.5 kPa.

However, one of the two promoted topographies had to be selected despite the correct prediction of the run-out distance. The shape comparison of the final deposition with the actual gave a clear advantage to the selection of the second alternative. The deposition of the first alternative had a slight turn to the right (Figure 28), contrary to the actual deposition which followed a straight path from the release area (Figure 24). On the other hand, the second topography simulated the landslide much better and the followed path was more realistic (Figure 29).

The comparison of other parameters such as maximum flow or average thickness gave no result because both topographies gave similar values over time. Furthermore, it was possible to approximate a rough estimation of the affected area from the sliding mass. Given the fact that the volume of the landslide was around 170000 m³ and the average thickness, after the completion of the displacement of the sliding mass, was around 1.2 meters, the affected area was 140000m². This is 40% higher than the actual landslide. As a result, despite the correct prediction of the run-out distance, the secondary parameters did not match so well with the actual ones. Consequently, other rheological models were sought.

6.3.2. Frictional Rheological Model

As far as the frictional rheological model is concerned, the selection of the parameters was the most difficult task. The determination of the pore-pressure coefficient (Ru) in particular proved to be more difficult than was expected for reasons, which are analytically described in the previous chapter. A wide range was selected in order to assure that the back-calculation would be representative. The best regeneration of the landslide event was given with the combination of a friction angle (φ) of 30 degrees and a coefficient pore-pressure (Ru) equal to 0.75. The results were close to reality and the comparison of the secondary results showed an amazing match.

Beyond the fact that the run-out distance was 510.1 meters, the shape of the deposition was similar to the actual one. Following the previously employed logic, the average thickness was around 1.8 meters and as a result, the affected area from the sliding mass was around 95000 m². This was only 5% less than the actual area and it could easily be neglected if all of the existing uncertainties are considered. A small variation in the velocity was observed between 30 and 60 seconds (Figure 31) and it was explained by topography since a small part from the sliding mass tended to slide to the right of the followed path (Figure 33).

6.4. Comparison of Models

Comparison between the results from NGI and the present study was one of the main goals of this thesis. NGI used software for the back-calculation of the landslide specially developed for submarine landslides, called BING3 (NGI 2017). A two-leveled comparison was conducted in order to have a realistic overview of the results. The first level was the direct comparison between the two different rheological models which were used in both analyses. The second was the utilization of the common parameters that NGI used for its simulation, on the rheological models of the present study.

Both the plastic and the frictional rheological models gave realistic results compared both with the actual case and with NGI results. The run-out distances were around 510 meters and the shapes of the final depositions were similar. However, the combinations of geotechnical parameters used in both analyses were different. It was expected that the combination would be different since the different rheological models demand different parameters and are governed by different rheological equations.

First, DAN3D's rheological models are simpler than BING3's, with less required geotechnical and rheological parameters. The Herschel-Bulkley rheological model requires a complex combination of both geotechnical and rheological parameters contrary to DAN3D. The direct utilization of BING3's parameters in DAN3D gave peculiar results. The sliding mass seemed to oscillate between the two opposite slopes (Figure 35). The fact that the shape of the final deposition was similar to the actual seems to be random rather than something solid. This was also concluded due to the fact that the average thickness was equal to 0.65 meters, showing the wide spreading of the sliding mass. Furthermore, the existence of two peaks at the velocity (Figure 35) justifies the conclusion that the sliding mass oscillated.

7. Conclusions and Recommendations for Further Work

7.1. Conclusions

The main task of the present study was the establishment of a set of parameters that could regenerate the landslide as realistically as possible. The utilization of the different rheological models led to the establishment of different sets of parameters for each rheological model. Both the plastic and the frictional rheological model gave realistic results (as described in Chapter 5). Based on the back-calculations and numerous analyses, the best combination for the regeneration of the landslide, given from the plastic rheological model, was with a shear strength equal to 8.5 kPa together with a unit weight of 16 kN/m³. The internal friction angle was set equal to 20 degrees for all analyses. The secondary results, such as velocity and average thickness showed that the sliding mass spread more than the actual deposit of the original landslide.

The frictional rheological model gave more accurate results in terms of the shape of the final deposition. The results from the secondary outputs were also represented. The combination which gave the best results, in terms of how realistically the landslide event was regenerated, had a friction angle equal to 30 degrees and a pore-pressure coefficient equal to 0.75. As in the previous model, the unit weight and the internal friction angle were 16 kN/m³ and 20 degrees respectively. The average thickness showed that the affected area was almost equal to the actual one in terms of space and shape.

Rheological Model	Plastic	Frictional
Unit Weight (γ) [kN/m³]	16	16
Internal Friction Angle (ϕ_i) [degrees]	20	20
Shear Strength (S_u) [kPa]	8.5	–
Fiction Angle (ϕ) [degrees]	–	30
Pore-Pressure Coefficient (R_u) [–]		0.75

Table 4: Table with the proposed values of the parameters which gave the most representative and realistic results in both rheological models.

Finally, the empirical approach of the landslide provided a good estimation of the run-out distance. Given that the prediction of the run-out distance was based on simple parameters, such as height of the slope or volume of the sliding mass, and that landslides are complex phenomena, the numerical calculation was deemed necessary if not mandatory. Additionally, the lack of empirical expressions for submarine landslides in calculation of the run-out distance renders the need for analytical calculation unavoidable.

The comparison between NGI (2017) and the present study showed that the back-calculation of the landslide with DAN3D gave similar results, even with simpler rheological models. However, the direct use of the parameters in different rheological models could give peculiar results. Consequently, either different sets of parameters must be used or calibration between two rheological models is necessary.

7.2. Further Work

The present study is not covering all aspects of the project. There are many more tasks to be done in order to have a complete and scientific overview of the stability of the seafloor in Bjørnafjorden. The proposed parameters should be used in the back-calculation of other landslides.

The back-calculation of other landslides in Bjørnafjorden could give other combinations of parameters which should be compared with the proposed from the present study and the differences should be discussed as well.

The present thesis studied the landslide using the plastic and the frictional rheological model. Consequently, other and more complicated models could also be used for the back-calculation of the same landslide. Rheologies, like Voellmy or Bingham, may regenerate the landslide more accurate and give a more realistic overview of its evolution.

Last but not least, DAN3D was used to back-calculate the landslide as a surficial landslide. As a result, more targeted software could be used, taking into account the drag force from the water resistance. For instance, NGI (2017) used BING3 for the back-calculation of the landslide. BING3 is specialized for the calculation of submarine landslides and parameters such as pressure drag coefficient C_p and friction drag coefficient C_{FR} are responsible for taking into account the water resistance.

7.3. Recommendations

Recommendations are addressed in two different directions. The first concerns the developers of DAN3D. The long simulation time is always a drawback for the selection of software. Despite the power of DAN3D as a tool, the time that the user had to spend on the obtaining of the results disallows them from selecting it. Furthermore, inconsistencies between the suggested default values from the software's manual and these on the software create a sense that the algorithm is not perfectly working and can mislead the user by providing inaccurate results.

The second recommendation concerns the user of DAN3D and those who want to use DAN3D for the simulation of either a surficial debris flow or a submarine landslide. Since topography plays a significant role in the configuration of the final result, the modification of it, according to the DAN3D's requirements, is a significant task and a careful estimation has to be made. The reliability of the conclusions of a study can be questioned if the inputted data are not corresponding to reality.

REFERENCES

Blasio, A., et al. (2004). "Flow models of natural debris flows originating from over consolidated clay materials." Marine Geology **213**: 439-455.

Blasio, F. V. D., et al. (2004). "Hydroplaning and submarine debris flows." JOURNAL OF GEOPHYSICAL RESEARCH **109**.

Brufau, P., et al. (2000). "1D mathematical modelling of debris flow " Journal of Hydraulic Research **38**: 435-446.

Coates, D. R. (1977). "Landslide perspectives." The Geological Society of America.

Cruden, D. M. and D. J. Varnes (1996). "Landslide Types and Processes." Transportation Research Board, U.S. National Academy of Sciences, Special Report, 247: 36-75.

Denlinger, R. P. and R. M. Iverson (2004). "Granular avalanches across irregular three-dimensional terrain: 1. Theory and computation." Journal of Geophysical Research **109**: F01014.

Gebreslassie, T. A. (2015). Dynamic simulations of landslide runout in cohesive soils. Department of Geosciences. Oslo, Norway, University of Oslo: 64.

Hungr, O. (1995). "A model for the runout analysis of rapid flow slides, debris flows and avalanches." Canadian Geotechnical Journal **32**: 610-623.

Hungr, O. (2010). "DAN3D Dynamic Analysis of Landslides in Three Dimensions Beta Version 2." 18.

Hungr, O., et al. (2014). "The Varnes classification of landslide types, an update." Landslides **11**(2): 167-194.

Hungr, O. and S. McDougall (2007). "Two numerical models for landslide dynamic analysis." Computers & Geosciences **35**: 978-992.

Imran, J., et al. (2001). "A numerical model of submarine debris flow with graphical user interface." Computers & Geosciences **27**: 717-729.

Kjennbakken, H., et al. (2017). Mapping and Modelling of Subsea Slides in Bjørnafjorden, Western Norway.

Leroueil, S., et al. (1996). Geotechnical characterization of slope movements. Special lecture.

Locat, J. and H. J. Lee (2000). "Submarine Landslides: Advances and Challenges." Proceedings of the 8th International Symposium on Landslides.

Mangerud, J. (2000). "Was Hardangerfjorden, western Norway, glaciated during the Younger Dryas?" NORSK GEOLOGISK TIDSSKRIF **80**.

McDougall, S. (2006). A new continuum dynamic model for the analysis of extremely rapid landslide motion across complex 3D terrain. Vancouver, Canada, University of British Columbia.

McDougall, S. and O. Hungr (2004). "A model for the analysis of rapid landslide motion across three-dimensional terrain." Canadian Geotechnical Journal **41**: 1084-1097.

McDougall, S. and O. Hungr (2005). "Dynamic modelling of entrainment in rapid landslides." Canadian Geotechnical Journal **42**: 1437-1448.

Meunier (1993). "Classification of stream flows. In: Proceedings of the Pierre Beghin International workshop on Rapid Gravitational Mass Movements." CEMAGREF: 231-236.

NGI (2016). Soil investigation - Data interpretation and evaluation of representative geotechnical parameters.

NGI (2017). Bjørnafjorden, straight floating bridge phase 3 Geohazard (Base Case).

Nigussie, D. G. (2013). Numerical modelling of run-out of sensitive clay slide debris. Department of Civil and Transport Engineering, Norwegian University of Science and Technology: 95.

Norem H., L. J. S. B. (1990). "An approach to the physics and the modelling of submarine landslides." Marine Geotechnology: 93-111.

Polykretis, C. (2013). Ανάπτυξη Μοντέλων Εκτίμησης της Επιδεκτικότητας για Εκδήλωση Κατολίσθησης με τη Χρήση Μεθόδων Γεωπληροφορικής και Τεχνητής Νοημοσύνης. Geography Department. Athens, Harokopio University: 17-33.

Pudasaini, S. P. and K. Hutter (2007). Avalanche Dynamics. Berlin.

Qarinur, M. (2015). "LANDSLIDE RUNOUT DISTANCE PREDICTION BASED ON MECHANISM AND CAUSE OF SOIL OR ROCK MASS MOVEMENT." Journal of the Civil Engineering Forum: 29-36.

Rickenmann, D. (1999). "Empirical Relationships for Debris Flows." Natural Hazards **19**: 47-77.

S., M. and O. Hungr (2003). "Objectives for the development of an integrated three-dimensional continuum model for the analysis of landslide runout.": In: Rickenmann, D., Chen, C.L. (Eds.), Proceedings of the Third International Conference on Debris-Flow Hazards Mitigation: Mechanics, Prediction and Assessment, Davos. Millpress, Rotterdam, pp. 481-490.

Savage, S. B. and K. Hutter (1989). "The motion of a finite mass of granular material down a rough incline

" Journal of Fluid Mechanics 199: 177–215.

Savage, S. B. and K. Hutter (1991). "The dynamics of avalanches of granular materials from initiation to runout ": Part1: Analysis. Acta Mechanica 86, 201–223.

Takahashi, T. (1991). "Debris Flow." International Association for Hydraulic Research monograph: A.A. Balkema, Rotterdam, 165pp.

Terzaghi, K. and R. B. Peck (1967). "Soil Mechanics in Engineering Practice." Wiley, New York, NY, 729pp.

Terzaghi, K. V. (1950). "Mechanisms of Landslides." Geotechnical Society of America: 83-125.

Thakur, V., et al. (2014). A preliminary study of rheological models for run-out distance modeling of sensitive clay debris. London, Taylor & Francis Group.

UNESCO (1990). "UNESCO Working Party on World Landslide Inventory." A suggested method for reporting a landslide. Bulletin of the International Association of Engineering Geology 41.

UNESCO (1993). "UNESCO Working Party on World Landslide Inventory." A suggested method for describing the activity of a landslide. Bulletin of the International Association of Engineering Geology 47.

Varnes, D. J. (1978). "Slope movement types and processes." In Special Report 176: Landslides: Analysis and control (Eds: Schuster, R.L and Krizek, R.J), Transportation and Road research board, National Academy of Science: 11-33.

Voellmy, A. (1955). "Über die Zerstörungskraft von Lawinen (On breaking force of avalanches)." Schweizerische Bauzeitung 73: 212-285.

Voight, B. and W. G. Pariseau (1978). "Rockslides and avalanches: an introduction." In: Voight, B.(Ed.), Rockslides and Avalanches, vol. 1. Elsevier, New York, NY, pp.1–67.

Yifru, A. L. (2014). Assessment of Rheological Models for Run-out Distance Modeling of Sensitive Clay Slides, Focusing on Voellmy Rheology. Department of Civil and Transport Engineering. Trondheim, Norway, Norwegian University of Science and Technology: 112.

Zaruba, Q. and V. Mencl (1969). "Landslides and their control." Elsevier: 205.

Zhan, W., et al. (2017). "Empirical prediction for travel distance of channelized rock avalanches in the Wenchuan earthquake area." Nat. Hazards Earth Syst. Sci., 17: 833-844.

APPENDIX

Model Grid Preparation (ASCII Format)

```
Path Topography.grd - Notepad
File Edit Format View Help
DSAA (1)
256 301 (2)
296623.328 297133.328 (3)
6667473.748 6668073.748 (4)
-551 -439 (5)
-512.1012 -512.3882 -512.5139 -512.7391 -512.9513 -513.1859 -513.4467
-516.2179 -516.4849 -516.7518 -517.0186 -517.2853 -517.5519 -517.8186
-520.4885 -520.7557 -521.0228 -521.2900 -521.5571 -521.8242 -522.0913
-524.7906 -525.0547 -525.2672 -525.4722 -525.6787 -525.8858 -526.0930
-527.9363 -528.1189 -528.3015 -528.4841 -528.6666 -528.8491 -529.0316
-530.0918 -530.0917 -530.0915 -530.0913 -530.0912 -530.0911 -530.0910
-530.0911 -530.0912 -530.0913 -530.0915 -530.0917 -530.0921 -530.0926
-528.6891 -528.4076 -528.1265 -527.8426 -527.5545 -527.2653 -526.9768
-523.9965 -523.6967 -523.3972 -523.0977 -522.7983 -522.4993 -522.2032
-519.5024 -519.2962 -519.0900 -518.8839 -518.6781 -518.4723 -518.2665
```

1. DSAA identifies the file as an ASCII grid file
2. Number of grid lines along x- and y-directions respectively (number of column & row lines)
3. Minimum and maximum x-values of the grid respectively
4. Minimum and maximum y-values of the grid respectively
5. Minimum and maximum z-values of the grid

All numbers under the fifth line represent the elevations of the surface every two meters. Each line of the grid is organized as a group of a 16x16 table.

